



NSTX

Structural Analysis of PF1, TF and OH Bus Bars

NSTX-CALC--55-01-02

Rev 1: August 1, 2014

Rev 2: June 20, 2015

Prepared By:

Andrei Khodak, Engineering Analyst

Reviewed By:

Peter Titus, Branch Head, Engineering Analysis Division

PPPL Calculation Form

Calculation # **NSTX-CALC-55-01-02** Revision # **02**

WP #, if any _____
(ENG-032)

Purpose of Calculation: (Define why the calculation is being performed.)

Perform Coupled Structural Electromagnetic and Thermal Analysis of PF1, TF, and OH bus bars

References (List any source of design information including computer program titles and revision levels.)

See attached report

Assumptions (Identify all assumptions made as part of this calculation.)

These are discussed throughout the attached report. Uncertainty of the friction of the bolted joint added in Rev 1 is addressed by varying the coefficient. Results were obtained for values of friction coefficients of 0.05, 0.10, 0.015, and 0.025. Stress results were similar beyond a friction factor of .05. It is assumed that the silver plated surfaces in the bolted lap joint have a friction factor above .05

Calculation (Calculation is either documented here or attached)

See attached Report

Conclusion (Specify whether or not the purpose of the calculation was accomplished.)

Results for PF, TF and OH bus bars summarized in the table below show that maximum values of stresses satisfy static structural design criteria.

Stress intensity in bus bars

<i>Coil connected to BusBar</i>	<i>Max Stress Intensity [MPa]</i>	<i>Max Stress Intensity in copper conductor [MPa]</i>
PF1A upper	205	205
PF1B upper	173	157
PF1C upper	111	71
PF1A lower	113	95
PF1B lower	107	98
PF1C lower	129	99
TF	172	172
OH	166	92

However maximum stress intensity in copper for PF1A, PF1B and TF bus bars is higher than fatigue design criteria of 125MPa. The areas of elevated stress are very small

For PF bus bars additional reinforcement measures were proposed which may eliminate this high stresses. This is analyzed in detail in PF part of center stack analysis report [3].

Maximum stress area for TF bus bar occurs in the area where conductor connection is assumed bonded. Actual bolted connection may allow more flexibility and reduce stress in the area.

Based on initial calculations insulated connectors are added between TF bus bars to reduce deflection.

Ground support of the TF bus bars was shifted to reduce stress from thermal expansion.

The thickness of the strait section of one of the TF bus bars was doubled to balance the electric current between two parallel bus bars, and correspondingly reduce maximum temperature.

Effect of friction in bolted connection was investigated using pretension of 50ksi and friction coefficients of 0.05, 0.10, 0.15, and 0.25. Stress intensity in copper conductors is reduced when friction is included; however local peaks of stress intensity appear at bolt holes edges. To reduce this stresses, chamfers on the bolt holes edges are recommended.

Resistance of the bus bar conductors was obtained from the analysis results, and presented in Table 6.

3/8 inch Inconel 718 high strength bolts should replace the 1/4-20 standard 316 bolts to support loads at the OH Coax terminal block . These are to be torqued to 43.5 ft-lbs . Belleville springs are to be included.

Cognizant Engineer's printed name, signature, and date

I have reviewed this calculation and, to my professional satisfaction, it is properly performed and correct.

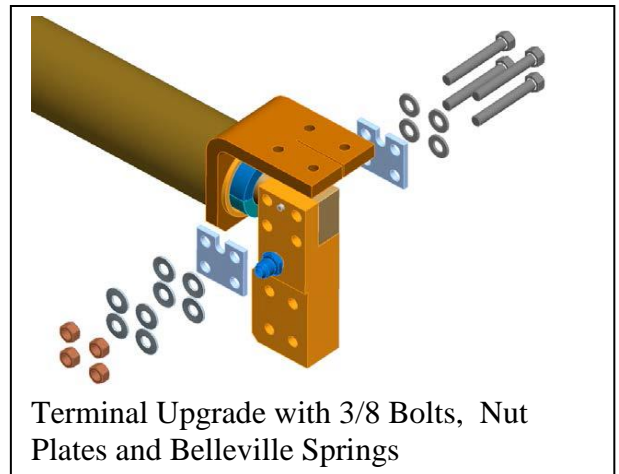
Checker's printed name, signature, and date

Executive Summary

Three-dimensional numerical simulations of PF1, TF, and OH bus bars were performed using ANSYS coupled solver for simultaneous structural, thermal and electromagnetic analysis. Thermal and electromagnetic simulations supported structural calculations providing necessary loads and strains. Simulations were performed during design process to verify structural integrity. Several major changes were introduced in the design of the bus bars since the initial report was submitted.

Results for PF, TF and OH bus bars show that maximum values of stresses satisfy static structural design criteria. However in some local small areas maximum stress intensity in copper for PF1A, PF1B and TF bus bars is higher than fatigue design criteria of 125MPa. For PF bus bars additional reinforcement measures were proposed which may eliminate this high stresses. This is analyzed in detail in PF part of center stack analysis report. Maximum stress area for TF bus bar occurs in the area where conductor connection is assumed bonded. Actual bolted connection may allow more flexibility and reduce stress in the area.

In Rev 2, an analysis of the OH Coax outer terminal block was added to qualify loads resulting from the bus bar analysis. 3/8 inch Inconel 718 high strength bolts replace the 1/4-20 standard 316 bolts to eliminate motion at the joint. These are to be torqued to 43.5 ft-lbs



Terminal Upgrade with 3/8 Bolts, Nut Plates and Belleville Springs

Introduction

The NSTX Center Stack Upgrade requires new bus bars for PF, TF, and OH coils, these bus bars are affected by Lorentz force since they are placed in a strong magnetic field and carry currents of up to 130kA. Thermal strains impose additional load on the bus bars since temperature of the bus bars is elevated during operation.

Scope of this Report

This report provides assessment of the structural integrity of bus bars based on Finite Element Analysis (FEA). Simulations were performed for the following for room temperature conditions.

The following parts of the coil assembly are included in the analysis:

- PF1A, B, C upper and lower bus bars with flags supports and parts of coil assembly
- OH bus bar together with coaxial part
- TF bus bars with supports and parts of connecting structure
- NSTX PF coils modeled as SOURCE36 elements
- NSTX TF coils modeled as SOURCE36 elements within the center stack, and as SOLID5 elements at the periphery

Revision History

Revision 02 of the report includes additional results on:

1. As-built configuration of the OH coax outer terminal. This begins on page 43

Revision 01 of the report includes additional results on:

1. Effect on friction in bolted joints on stress in copper parts. The location of the bolted connection is shown in figure 24c, and results begin at figure 25e Resistance of the bus bar conductors was added in Table 6 page 36
2. Resistance of the bus bar conductors was added in Table 6 page 36
3. Conclusions moved to PPPL Calculation Form
4. Added plots for stress intensity in copper conductors
5. Formatting of figures, units added

Mathematical Model

Geometry

Design geometry

Details of the design model of the CS insert coil are presented on Fig.1. The model was designed using Pro/Engineer CAD software. Model and mesh of the parts 1,2,3,4 was provided by H. Zhang.

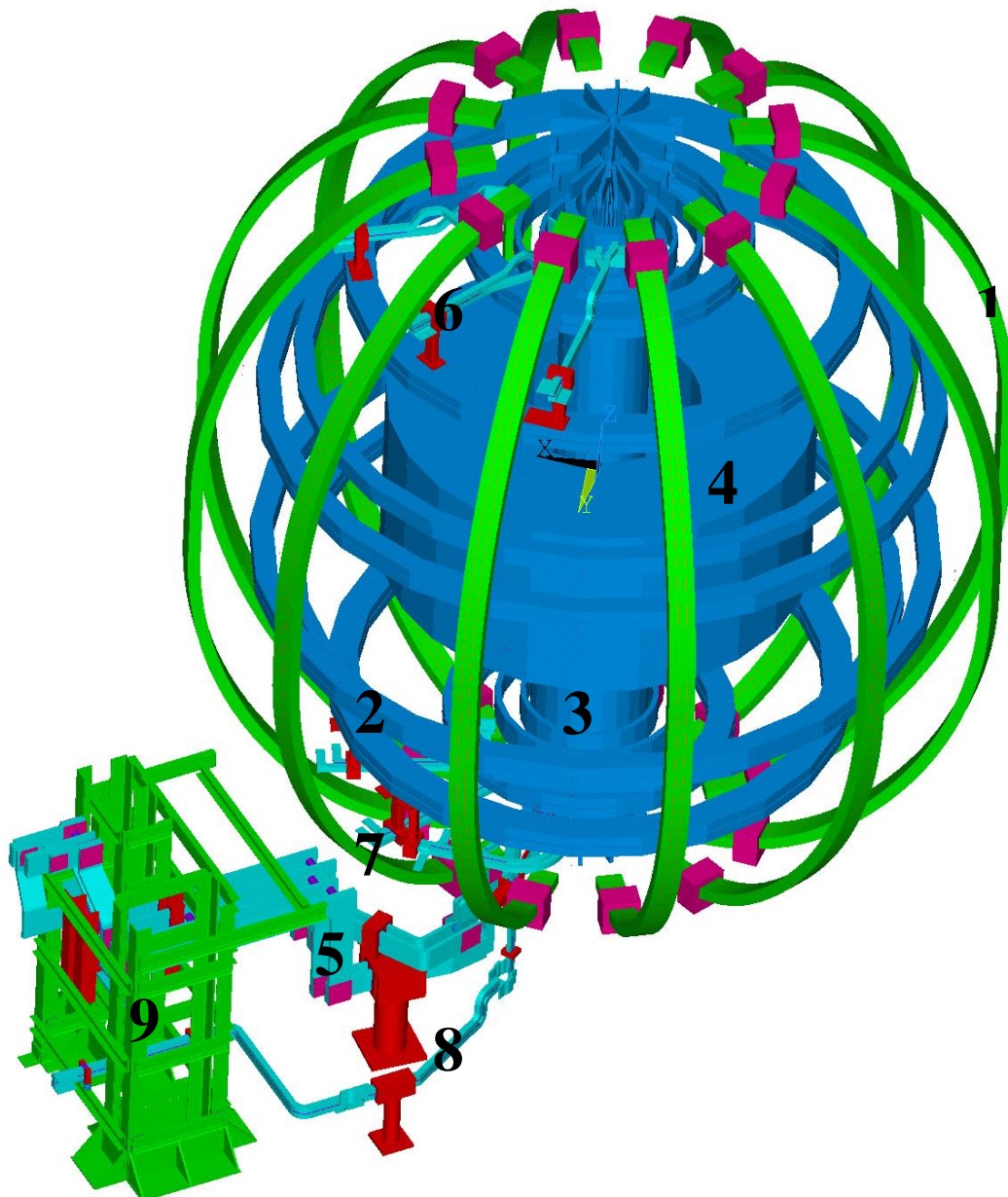


Fig1. Design model of the NSTXU coils and bus bars:

1. TF coils
2. PF coils
3. OH coils

4. Plasma
5. TF bus bars
6. Upper PF bus bars

7. Lower PF bus bars
8. OH bus bar
9. Support tower

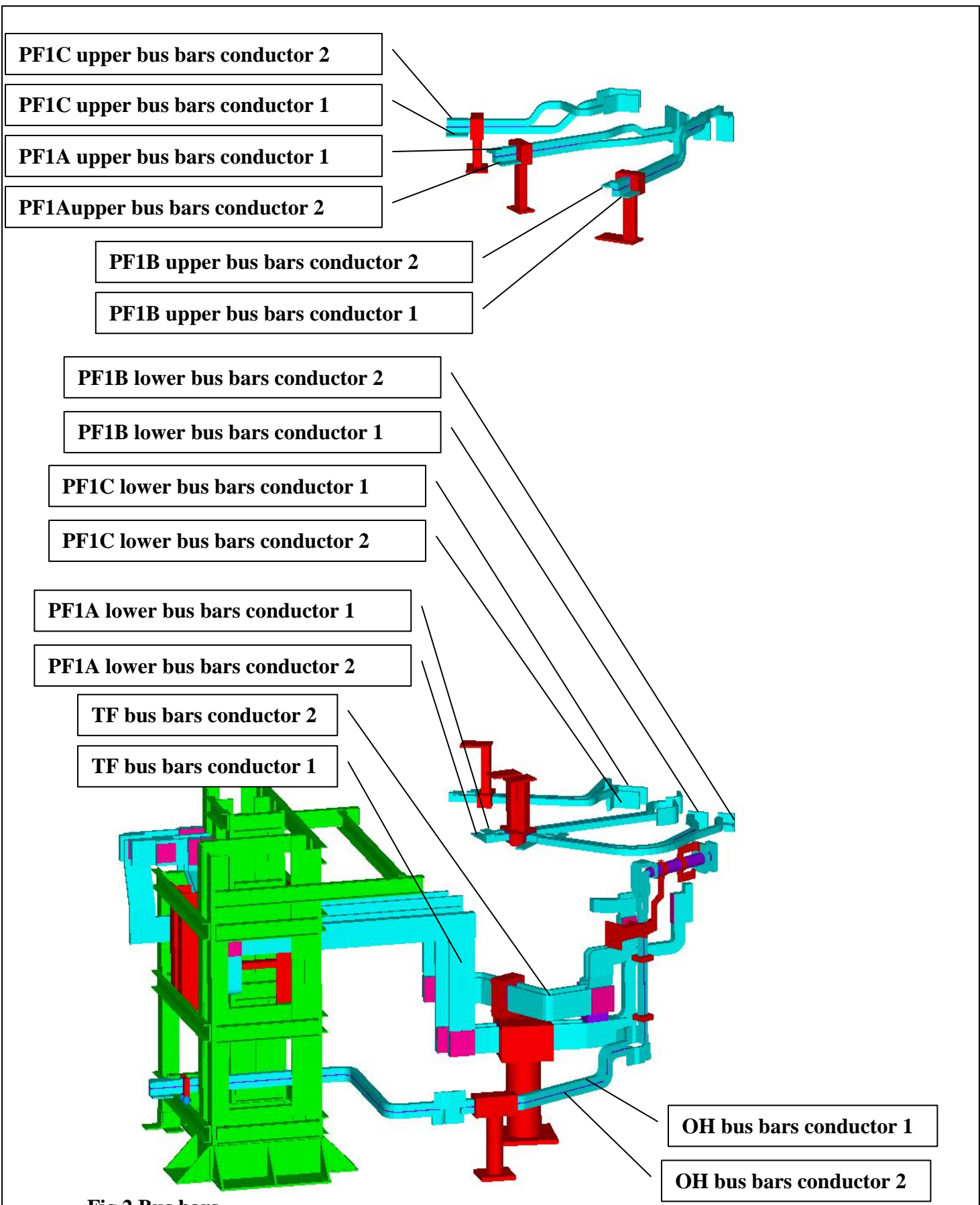


Fig 2. Bus bars

Bus bars analyzed in present investigation are presented on fig.2. PF bus bars were modeled together with a portion of the coils to insure proper loads on flags.

Geometry Simplification

Geometry simplification was performed using Pro/Engineer software mostly by deleting features in the original design model. Initial design geometry was simplified for the purpose mesh generation by removing some of the fillets from the design. The effect of the fillets is only to reduce peak stresses (a beneficial trait) and their contribution to the global stiffness of the structure is negligible. Most of the bolt connections of the bus bar supports were also removed and bonded connection was assumed.

The model was modified further using ANSYS Workbench Design Modeler software. Geometry was imported from Pro/Engineer into Design Modeler via IGES file. Modifications of TF bus bar supports are shown on fig 3.

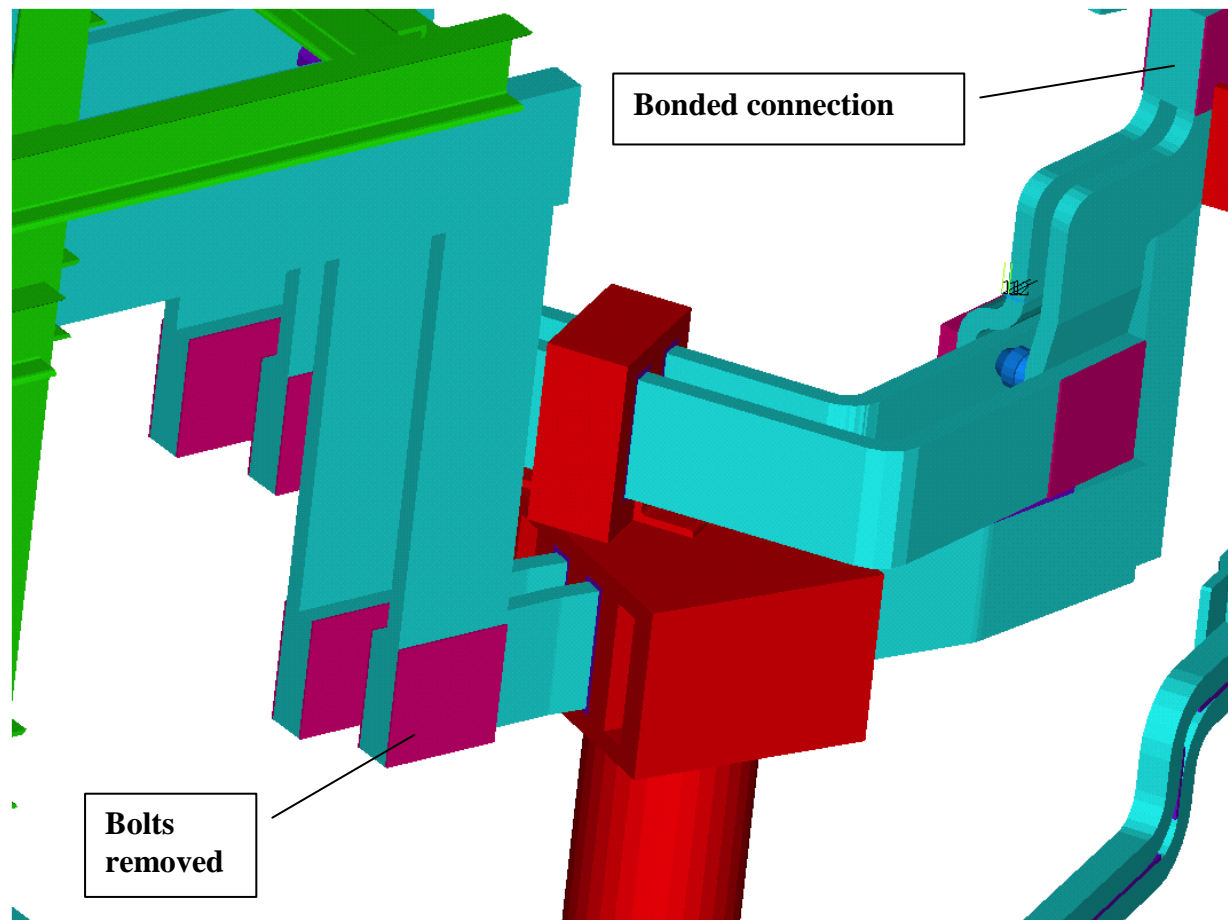


Fig 3 TF bus bar supports modification

Meshing

Elements used

ANSYS elements used to mesh the model are presented in Table 1. SOLID5 elements were used for model geometry meshing. SOLID5 elements allow simultaneous solution for coupled structural, thermal, and static electro-magnetic problem. The volumes that could not be measured with structural brick elements we meshed with unstructured mesh using SOLID 226 tetrahedral elements

Source elements were used to create external magnetic field.

Bolt friction analysis included pretension in bolts, and friction between copper parts. In this analysis contact and pretension elements are used

Table 1 Elements used in the FE Model

Element Type	Nodes	Name	Used in the Mesh of
3-D Coupled Solid	8	SOLID5	Majority of parts
3-D Structural Solid	4	SOLID226	Parts with unstructured mesh
Source	2	SOURCE36	External Magnetic Field
3-D Node-to-Node Contact	2	CONTA178	Contact friction for bolt connection
Pretension	3	PRETS179	Pretension for bolt friction analysis

Geometry split into blocks

SOLID5 ANSYS elements require using sweep method for meshing. Thus, the model has to be split into blocks that can be swept. The model was split within ANSYS Classic. Splitting of the model into blocks does not introduce any additional geometrical simplifications into model, and was used exclusively for meshing simplification Example of the geometry split into multiple blocks is presented on Fig 4.

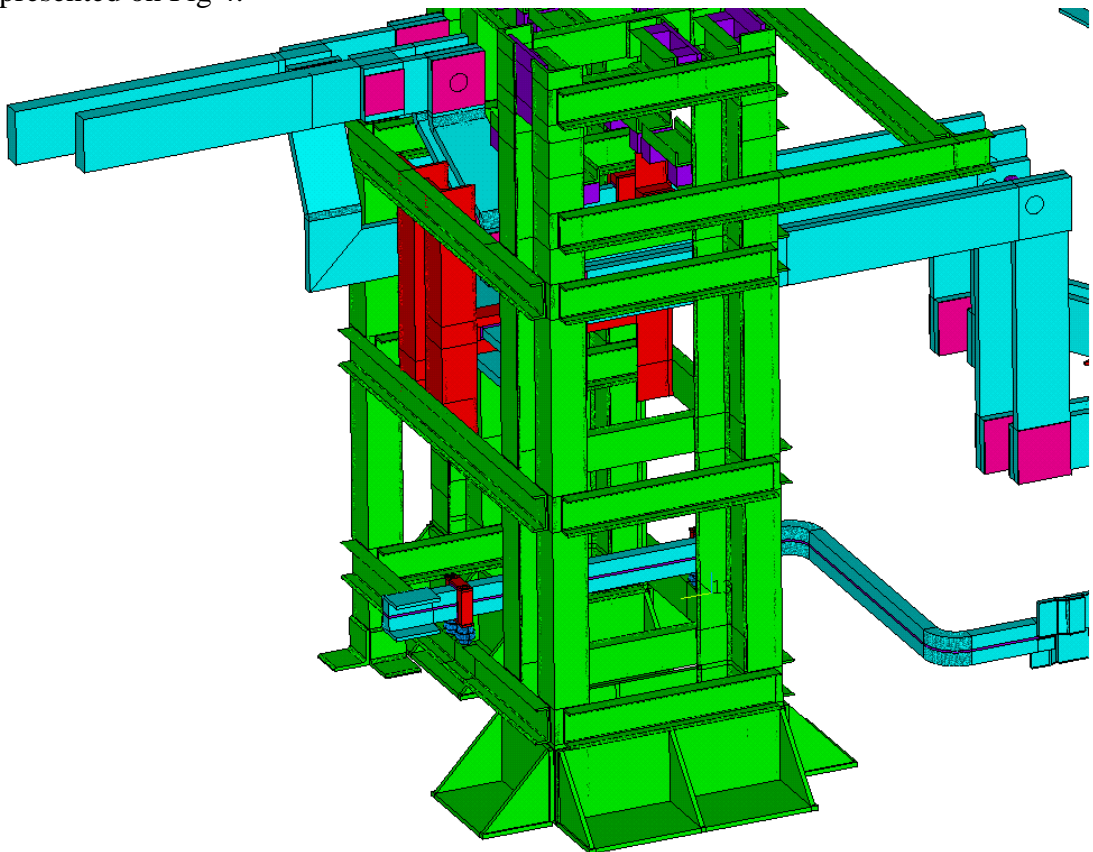


Fig 4 Splitting of TF bus bar model allowing hexahedral sweep meshing

Meshing

Meshing was performed within standalone version of ANSYS. Final mesh containing 378981 elements is presented on Fig 6, 7, and 8.

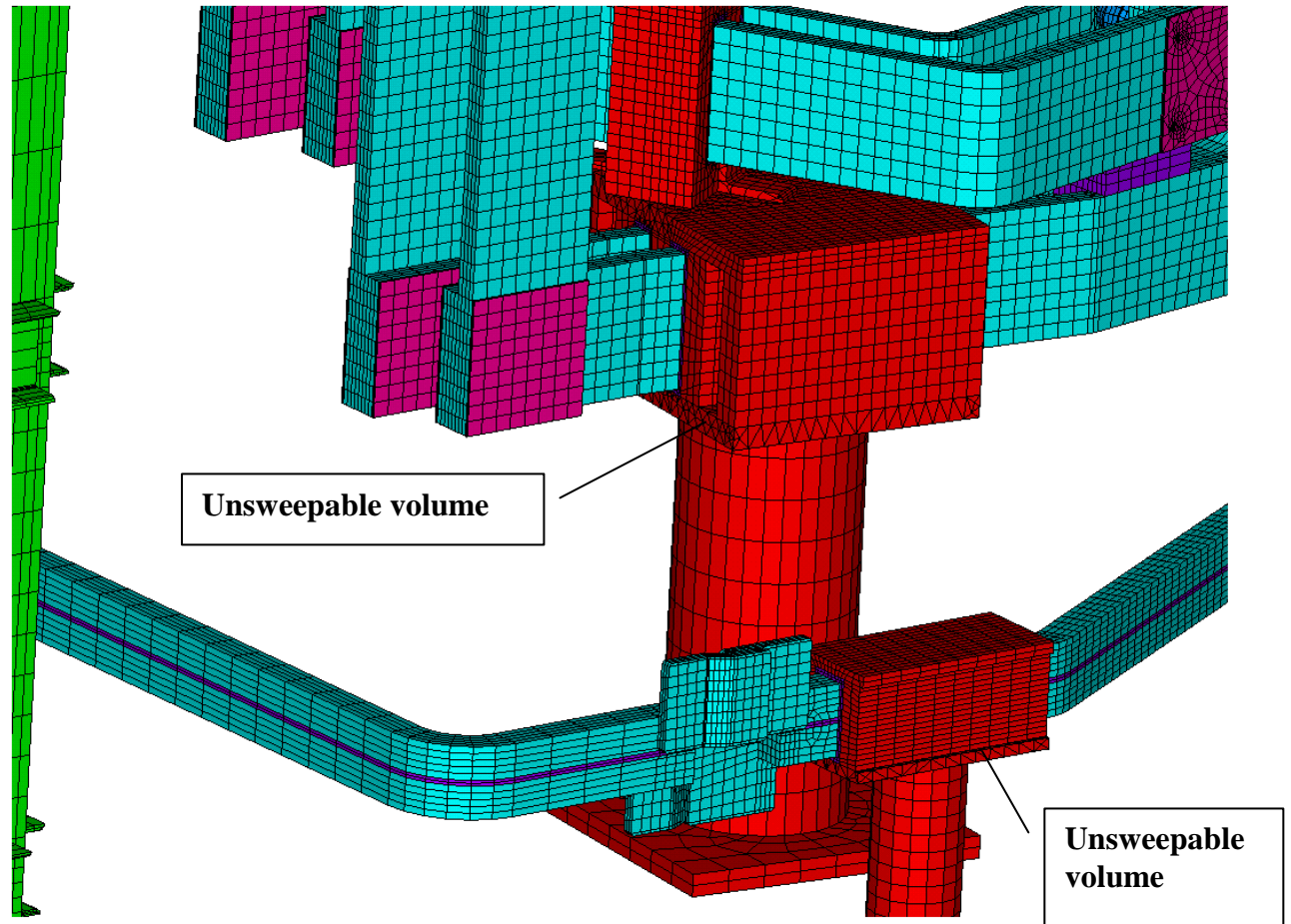


Fig 6 Mesh for TF bus bars

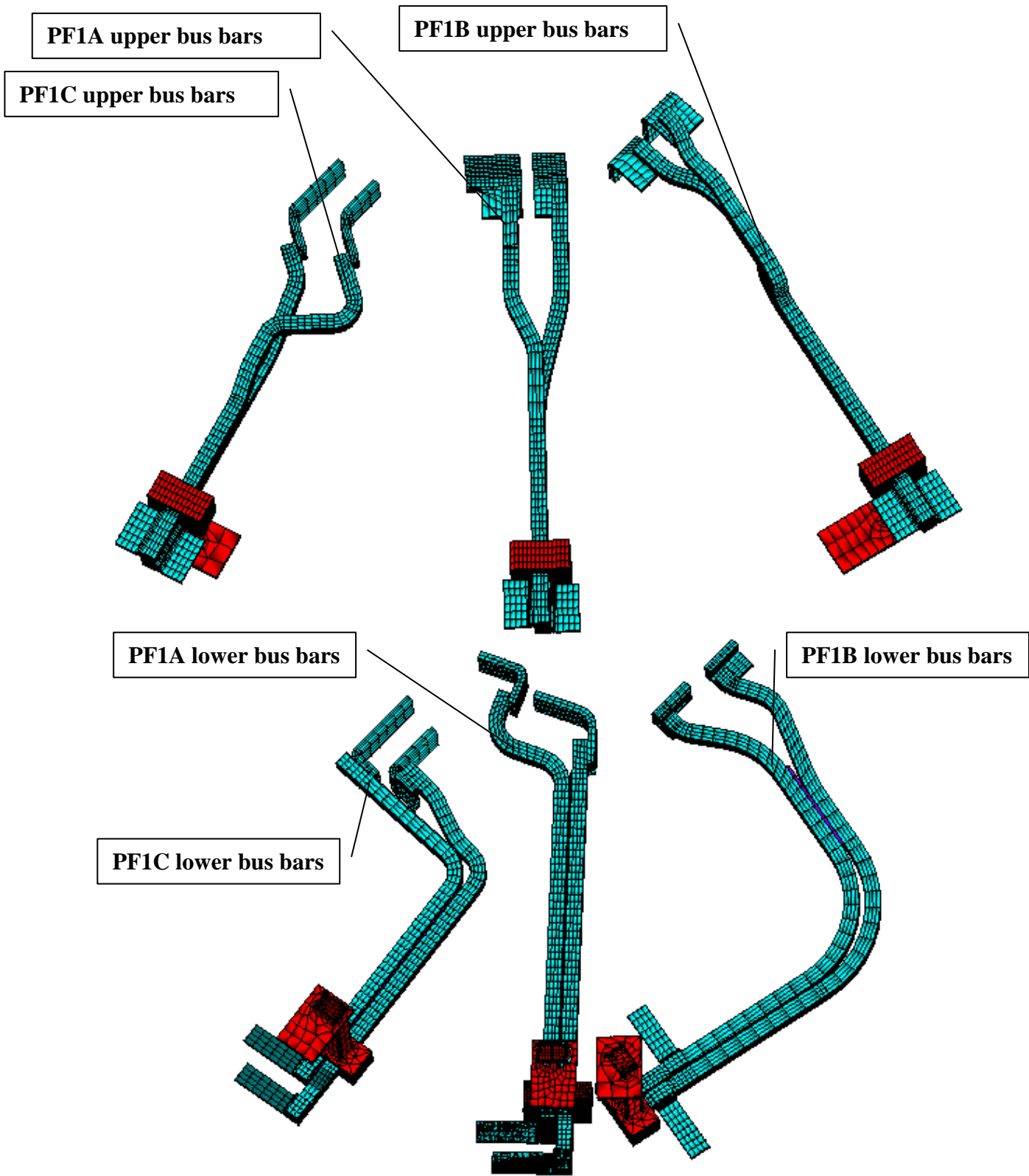


Fig 7 Mesh for PF bus bars

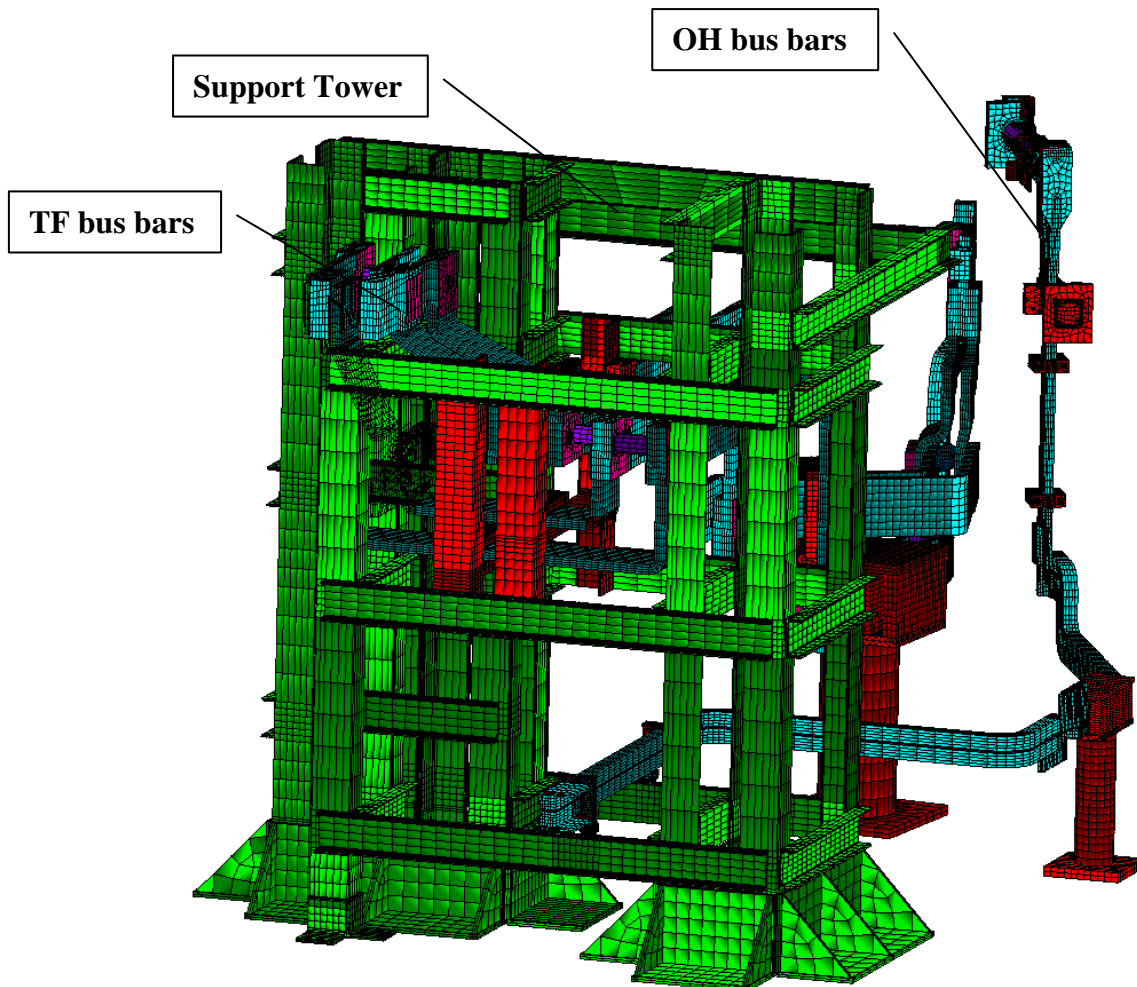


Fig 8 Mesh for TF and OH bus bars with support tower

Boundary Conditions and Loads

Structural boundary conditions

The model is fixed in all directions as shown on fig 9. Supporting brackets are fixed in places of attachment to other structures. Both ends of the OH bus bars are fixed, as well as outer ends of the TF bus bars. Inner TF bus bar directly connected to outer portion of the TF coil (see fig 9). The other TF bus bar is fixed at center stack connection. Most of PF bus bars are fixed at the flags with no displacement. Positive vertical displacement of 1 cm is imposed on PF1A, and PF1B flags. Analysis of center stack thermal expansion was provided by A. Brooks. Outer ends of PF bus bars are not fixed since they are attached to flexible connectors.

Connected directly to
TF coil model

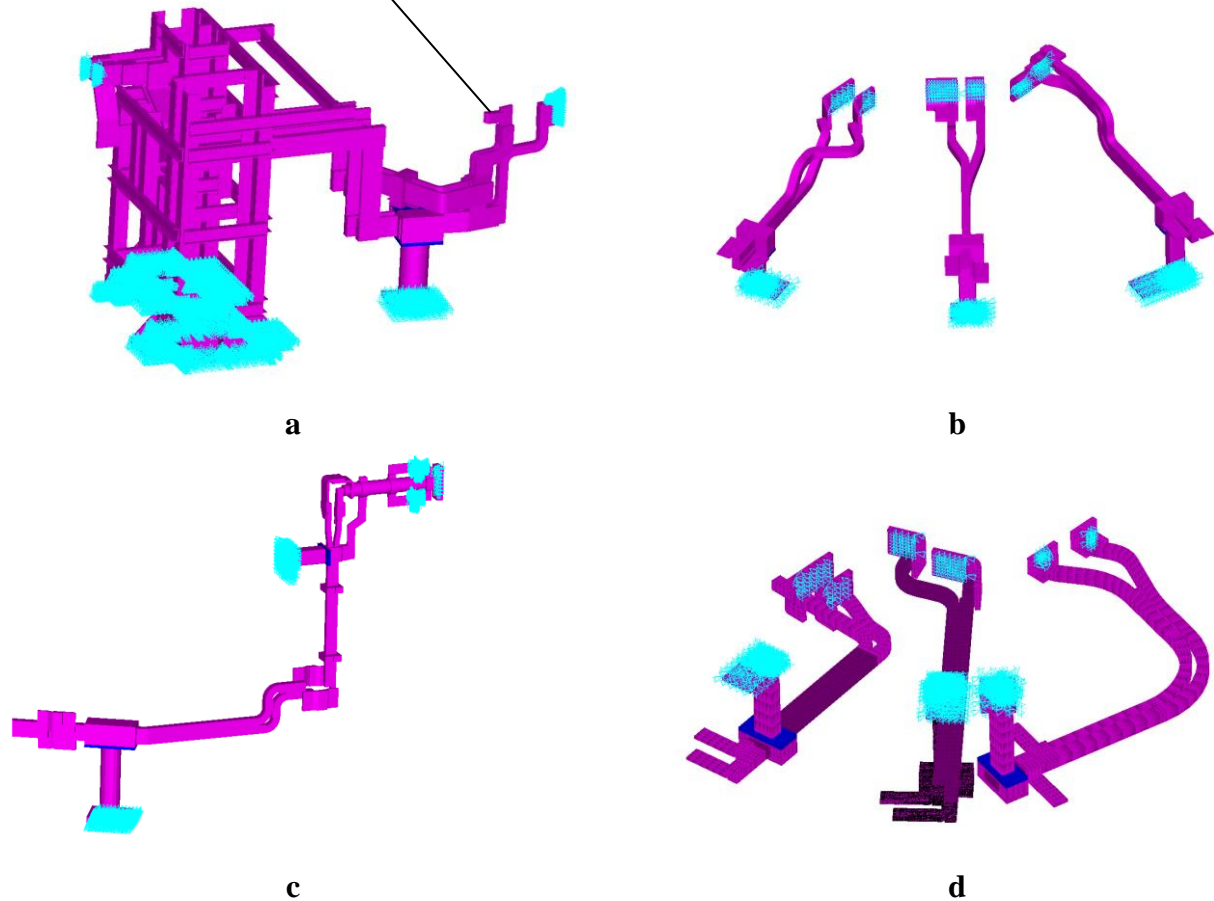


Fig 9 Structural boundary conditions a) TF bus bars; b) Upper PF bus bars c) OH bus bar; d) Lower PF bus bar

Thermal Load

Constant temperature boundary conditions are summarized in table 2. Cooling channels of TF and OH buses are presented on fig 10.

Table 2 Constant temperature boundary conditions

Part	Side	Temperature
OH bus bars	outer	40 °C
	center stack	40 °C
	cooling channels	20 °C
TF bus bars	outer	50 °C
	outer TF coil	50 °C
	center stack	40 °C
PF bus bars	cooling channels	20 °C
	outer	40 °C
PF bus bars	center stack	100 °C
	fixed points	35 °C

Reference temperature of 20 °C was used for thermal strain calculation, as a temperature during assembly, of the device. Heat transfer conditions were imposed on the all external walls with film coefficient of 7 and ambient temperature of 35 °C

TEMP

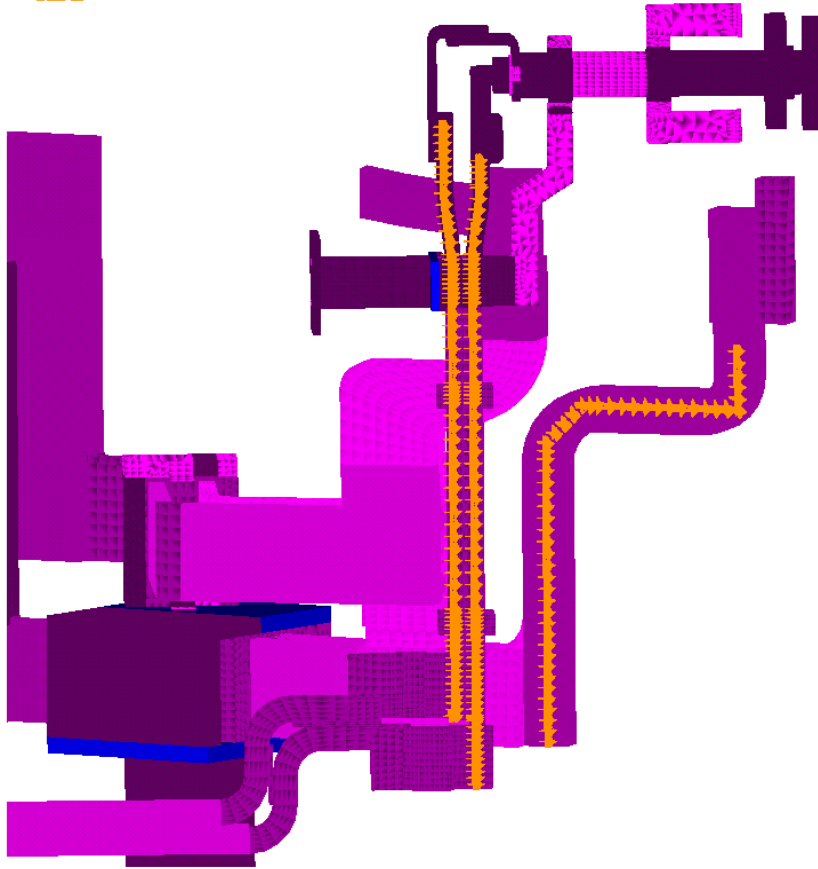


Fig 10 Cooling channel walls at 20 °C or OH and TF bus bars

With this boundary conditions heat transfer problem was resolved including Joule heat on the conductor parts. However resistivity of copper was assumed 150 times lower to model 8s pulse every 20 minutes.

Electric Boundary Conditions

Electrical boundary conditions were imposed on the opposing ends of the each bus bar cable, to simulate constant electrical current flow. At one end constant voltage level of zero was imposed, while on the other end constant current level corresponding to the coil and scenario is imposed. The current direction in bus bars is chosen in consistence with correspondent coil current direction. Scenario 72 was chosen to obtain current values. In this scenario all PF1 coils are charged at maximum values, and higher values are also imposed on PF4 and PF5 coils creating strong magnetic field. Currents used to charge coils and corresponding bus bars are presented in table 3:

Table 3

Coil	PF1AU	PF1BU	PF1CU	PF2U	PF3U	PF4	PF5	PF3L	PF2L	PF1CL	PF1BL	PF1AL	OH	TF
Current [kA]	18.3	13	15.9	15	-16	-16	-34	-16	15	15.9	13	18.3	-24	130

External magnetic Field

External to bus bars magnetic field was generated using SOURC36 elements for PF and OH coils and inner parts of TF coil, outer legs of TF coils were meshed using SOLID5 elements as shown fig. 12. The model was provided by Han Zhang. The values of the parameters used for source elements are summarized in the table 4. They correspond to the Scenario 72 and create external field presented on fig. 12. Axial field of more than one Tesla is assumed conservative approximation of all the scenario effects on the bus bars.

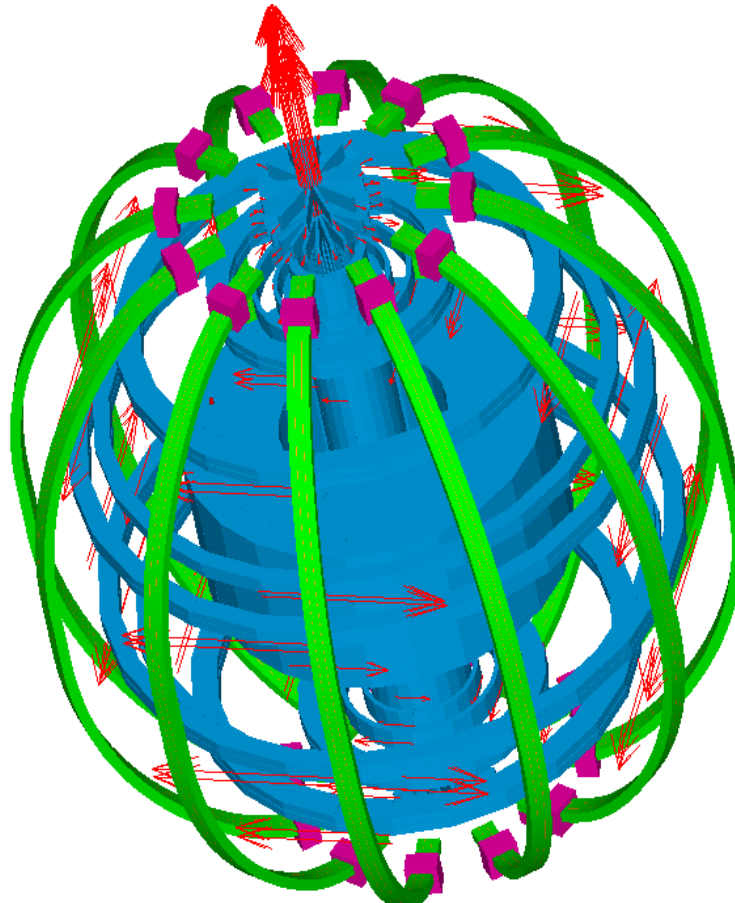


Fig 11 External magnetic field creating elements

Table 4 Magnetic field source element properties

Coil	R (center) (cm)	dR (cm)	Z (center) (cm)	dZ (cm)	nR	nZ	Turns
OH (half-plane)	24.2083	6.9340	106.0400	212.0800	4.0	110	442
PF1a	32.4434	6.2454	159.0600	46.3296	4.0	16	64
PF1b	40.0380	3.3600	180.4200	18.1167	2.0	16	32
PF1c	55.0520	3.7258	181.3600	16.6379	2.0	10	20
PF2a	79.9998	16.2712	193.3473	6.7970	7.0	2	14
PF2b	79.9998	16.2712	185.2600	6.7970	7.0	2	14
PF3a	149.4460	18.6436	163.3474	6.7970	7.5	2	15
PF3b	149.4460	18.6436	155.2600	6.7970	7.5	2	15
PF4b	179.4612	9.1542	80.7212	6.7970	2.0	4	8
PF4c	180.6473	11.5265	88.8086	6.7970	4.5	2	9
PF5a	201.2798	13.5331	65.2069	6.8580	6.0	2	12
PF5b	201.2798	13.5331	57.8002	6.8580	6.0	2	12

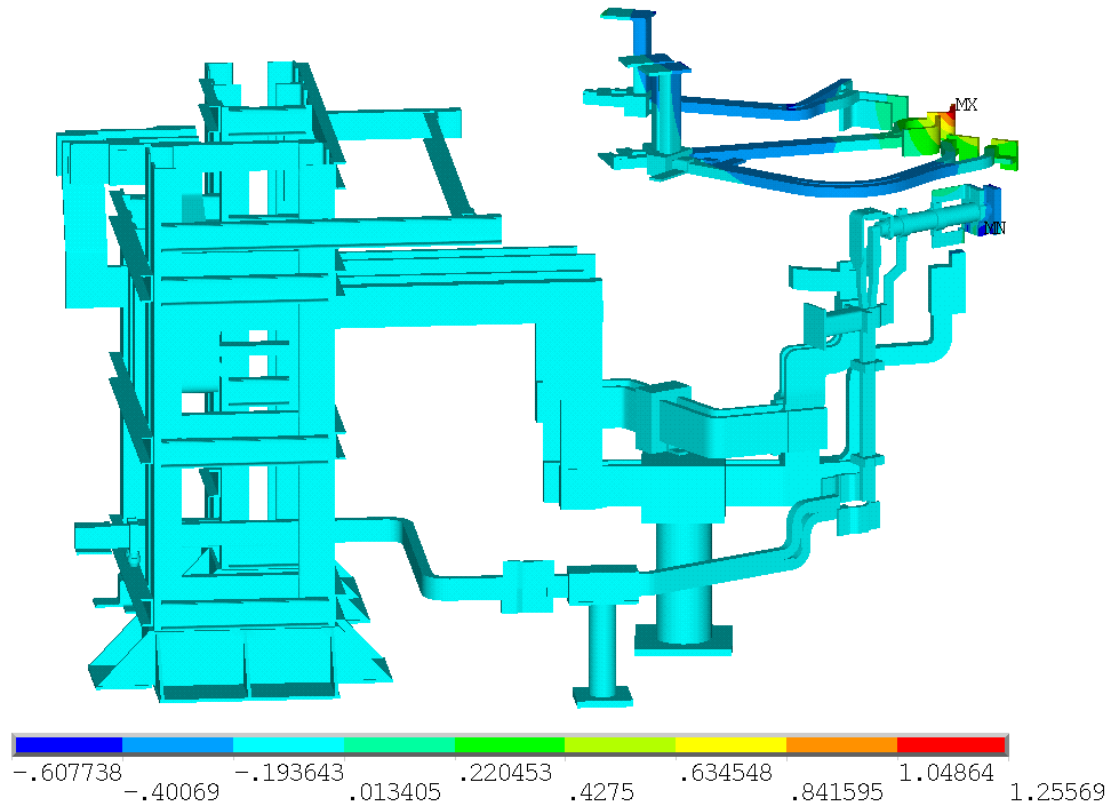


Fig 12.a Axial component of external magnetic field [Tesla]

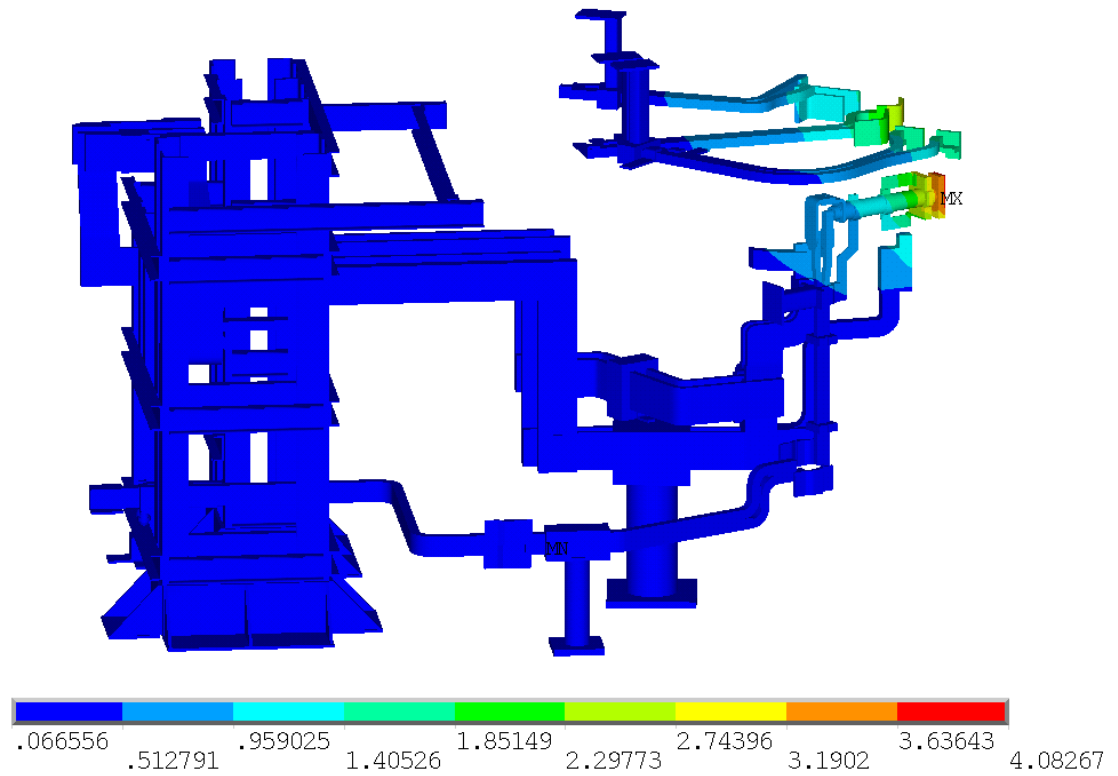


Fig 12.b Toroidal component of external magnetic field [Tesla]

Material properties for bus bar analysis model

Conductors

Material: copper.

Material is isotropic with elastic modulus of 120GPa and Poisson ratio of 0.33.

Thermal conductivity is 385[W/(mK)].

Thermal expansion coefficient is $1.64 \cdot 10^{-5}$ [1/K] at 293K.

Temperature dependent electrical resistivity is presented in table 5. Value used in analysis was 150 times less assuming 8s pulse in 20 min interval

Table 5 Copper conductor electrical resistivity

Temperature°C	273	293	393
r_{Cu} [Ωm]	1.49E-08	1.62E-08	2.28E-08
r_{Cu} [Ωm] used in analysis	9.91E-11	1.08E-10	1.52E-10

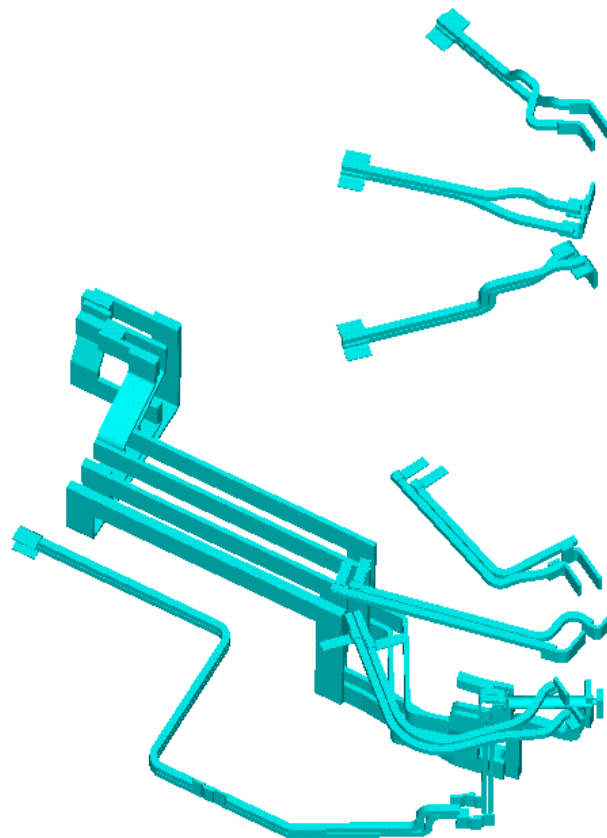


Fig 13 Copper conductors

Insulation

Material: G10.

Material is isotropic with elastic modulus of 20GPa and Poisson ratio of 0.33.

Thermal conductivity is 0.288 [W/(mK)].

Thermal expansion coefficient is $0.99 \cdot 10^{-5}$ [1/K] at 293K.

Electrical resistivity is $1.673 \cdot 10^{+6}$ [Ohm·m]



Fig 14 Insulation

Support Hardware

Material: steel.

Material is isotropic with elastic modulus of 190GPa and Poisson ratio of 0.33.

Thermal conductivity is 25[W/(mK)].

Thermal expansion coefficient is $1.60 \cdot 10^{-5}$ [1/K] at 293K.

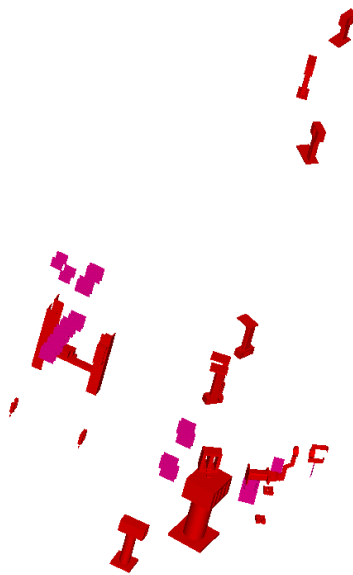


Fig 15 Supporting Hardware

Insulating Inserts

Material: insulating plastic.

Material is isotropic with elastic modulus of 20GPa and Poisson ratio of 0.

Thermal conductivity is 0.288 [W/(mK)].

Thermal expansion coefficient is $1.6 \cdot 10^{-5}$ [1/K] at 293K.

Electrical resistivity is $1.673 \cdot 10^{+6}$ [Ohm·m]

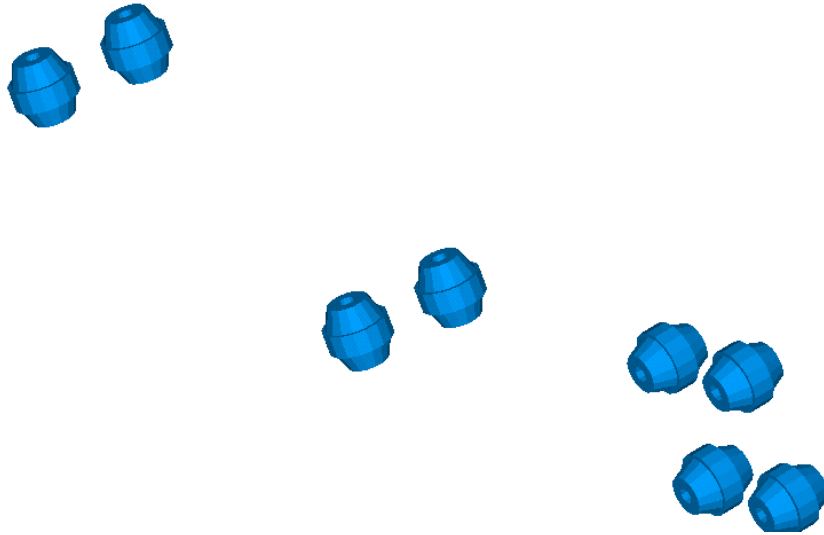


Fig 16 Insulating inserts

Compressible Inserts or PF1A upper and PF1B upper supports

Material: insulating plastic.

Material is isotropic with elastic modulus of 150MPa and Poisson ratio of 0.49

Thermal conductivity is 0.288 [W/(mK)].

Thermal expansion coefficient is $0.99 \cdot 10^{-5}$ [1/K] at 293K.

Electrical resistivity is $1.673 \cdot 10^{+6}$ [Ohm·m]



Fig 17 Compressible inserts

Support Tower

Material: Aluminum 6061

Material is isotropic with elastic modulus of 68.9GPa and Poisson ratio of 0.33.

Thermal conductivity is 167 [W/(mK)].

Thermal expansion coefficient is $2.36 \cdot 10^{-5}$ [1/K] at 293K.

Electrical resistivity is $3.99 \cdot 10^{-8}$ [Ohm·m]

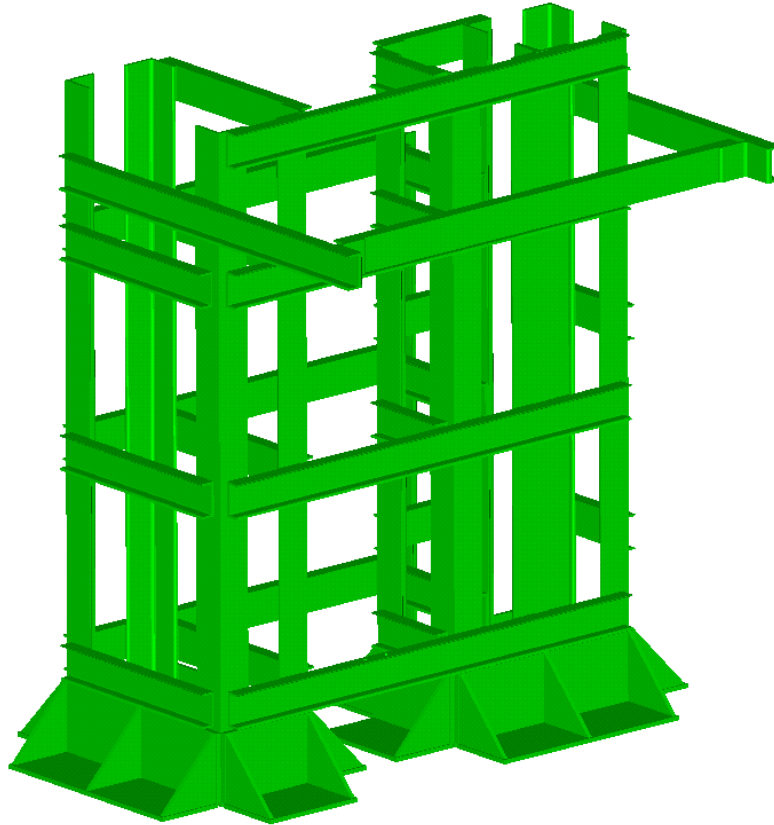


Fig 18 Supporting Tower

Simulation Results

PF Upper Bus Bars

PF1A Upper Bus Bar

Stress intensity and displacements on PF1A upper bus bar are presented on Fig. 19

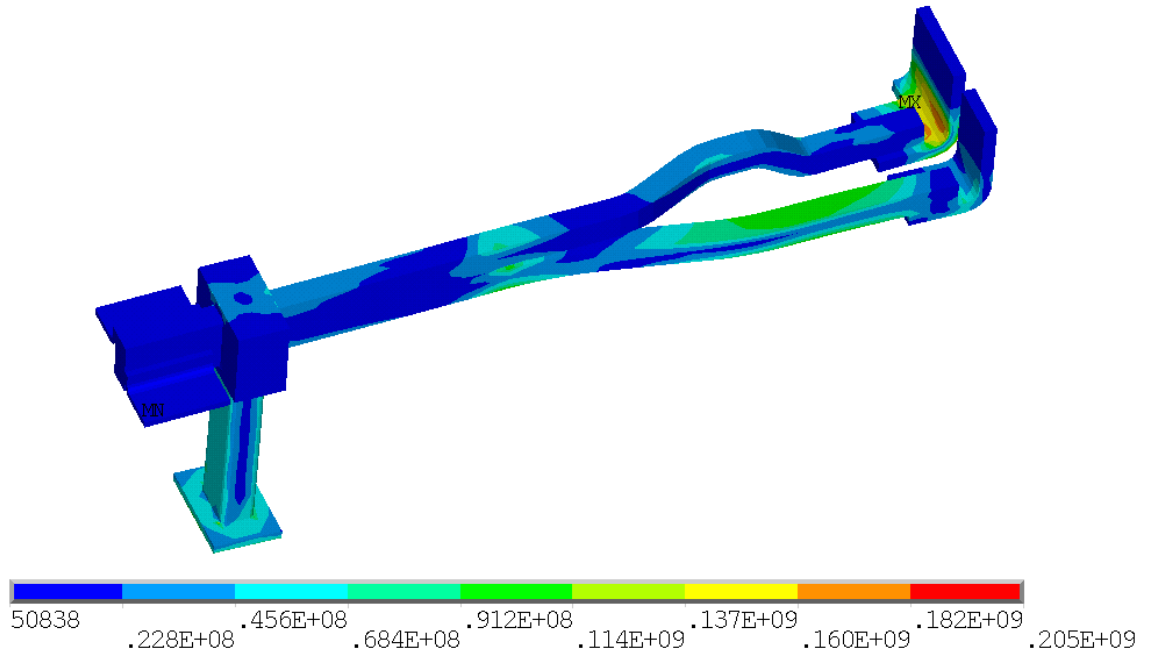


Fig 19.a Stress intensity [Pa]

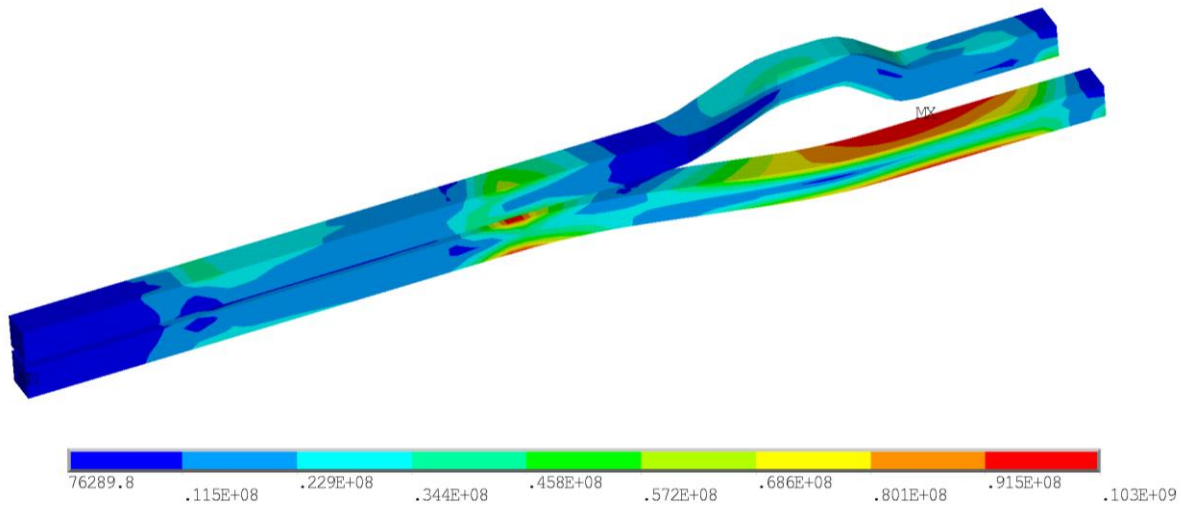


Fig 19.b Stress intensity in copper conductor [Pa]

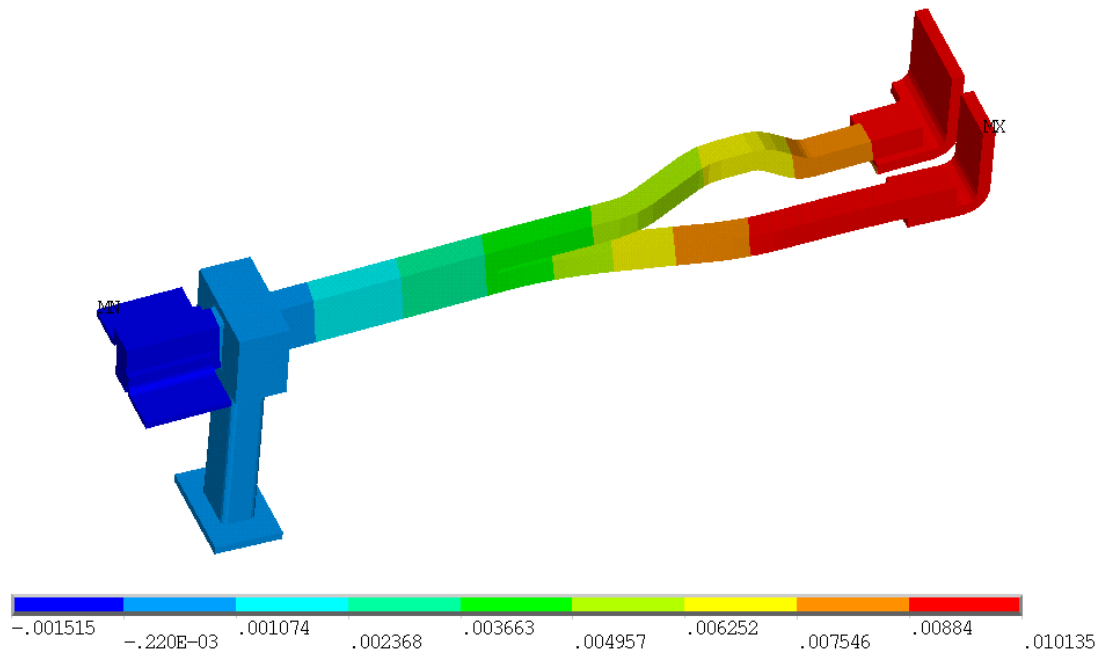


Fig 19.c Vertical Displacement [m]

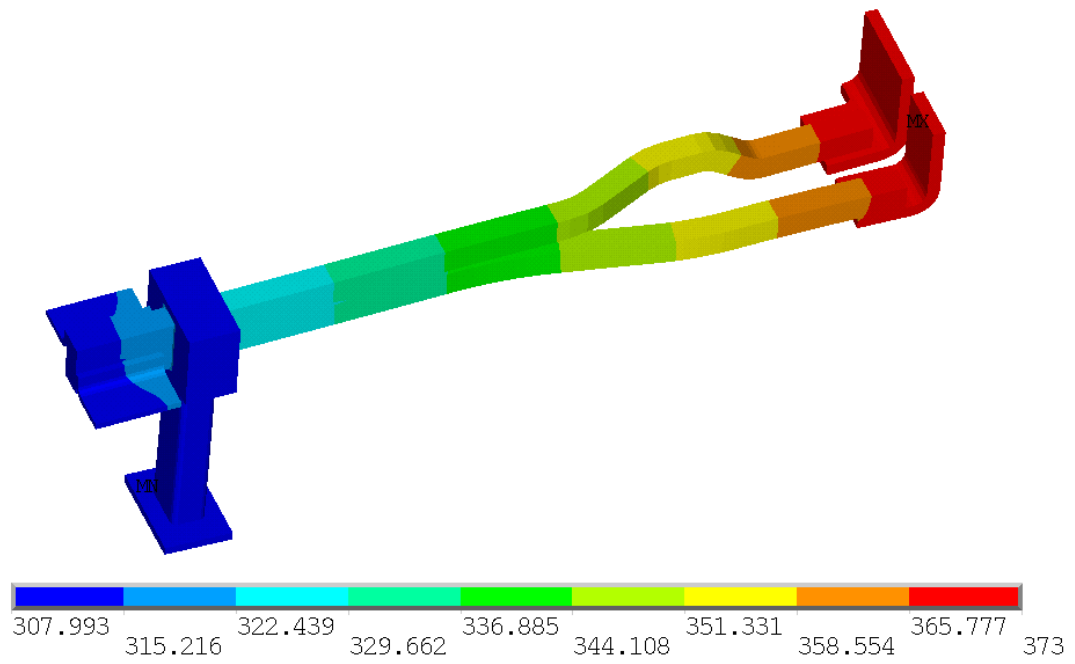


Fig 19.c Temperature [K]

PF1B Upper Bus Bar

Stress intensity and displacements on PF1B upper bus bar are presented on Fig. 20

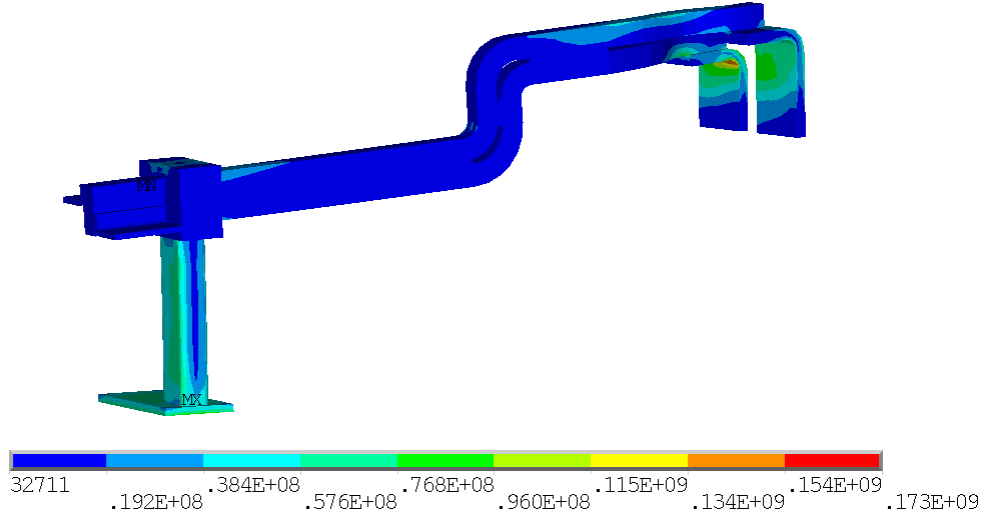


Fig 20.a Stress intensity [Pa]

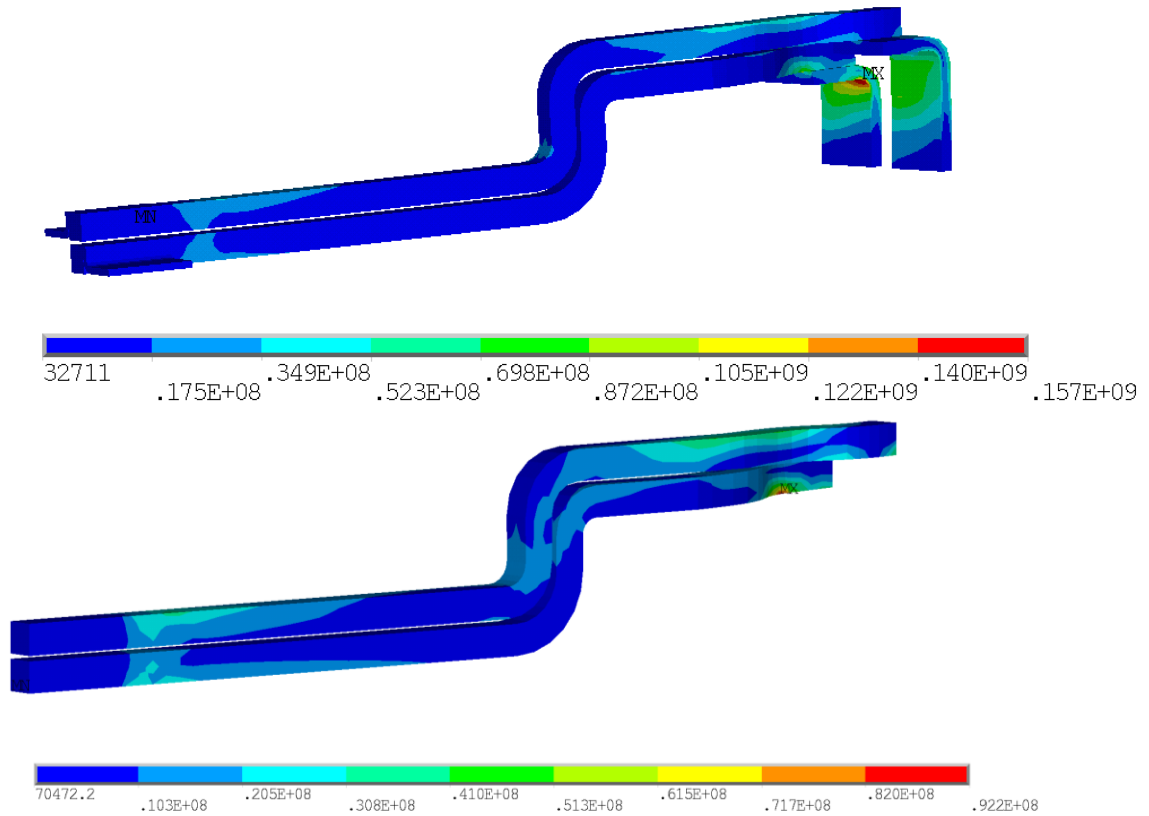


Fig 20.b Stress intensity in copper conductor [Pa]

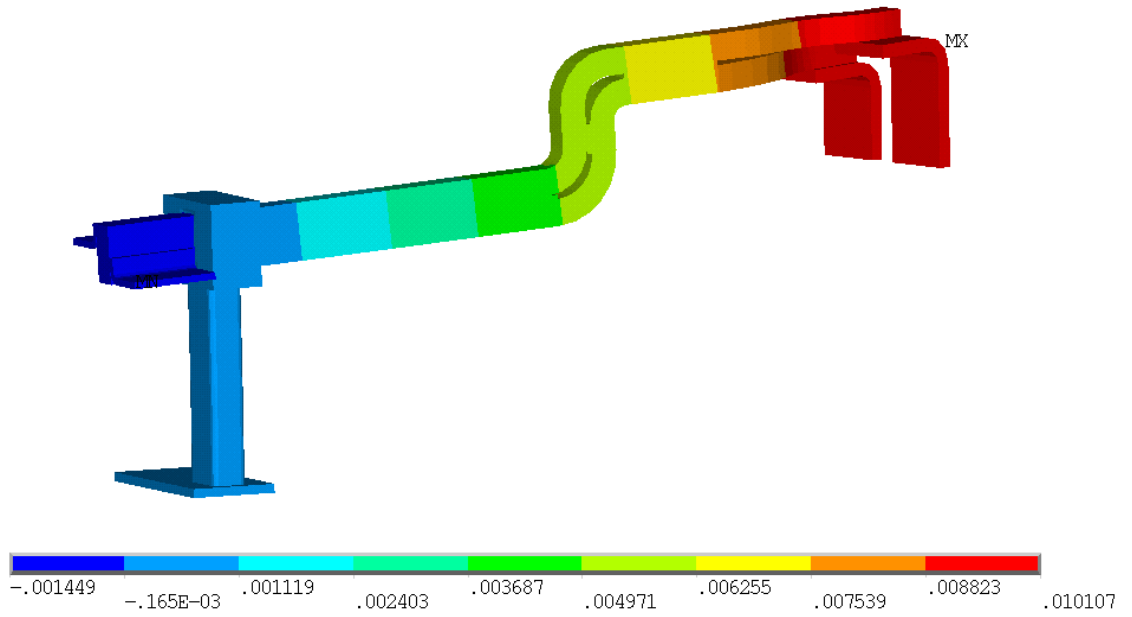


Fig 20.c Vertical Displacement [m]

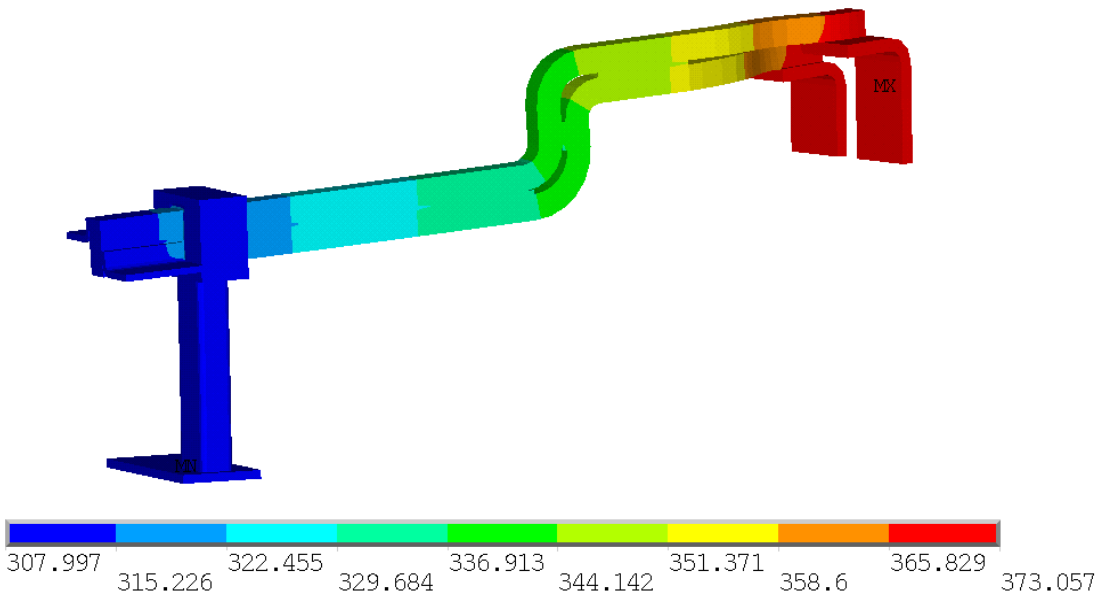


Fig 20.d Temperature [K]

PF1C Upper Bus Bar

Stress intensity and displacements on PF1C upper bus bar are presented on Fig. 21

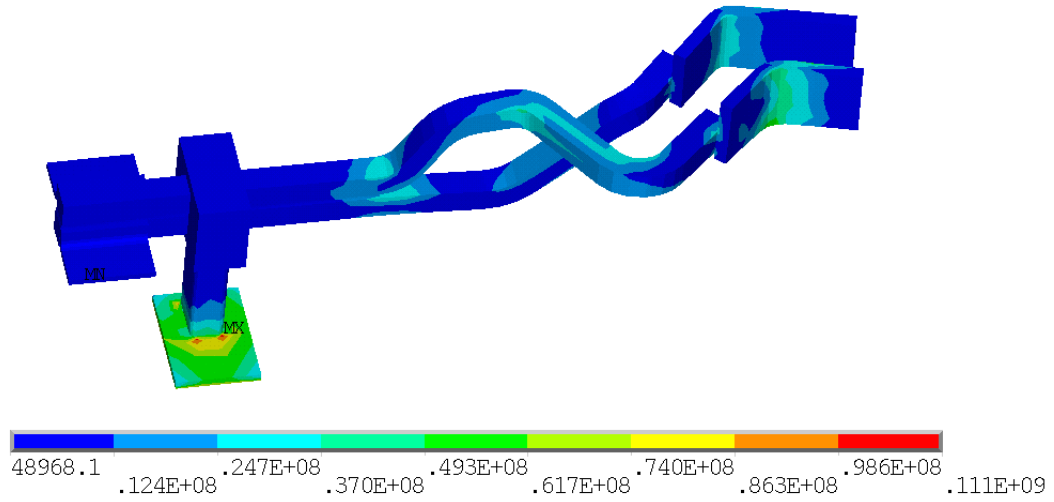


Fig 21.a Stress intensity [Pa]

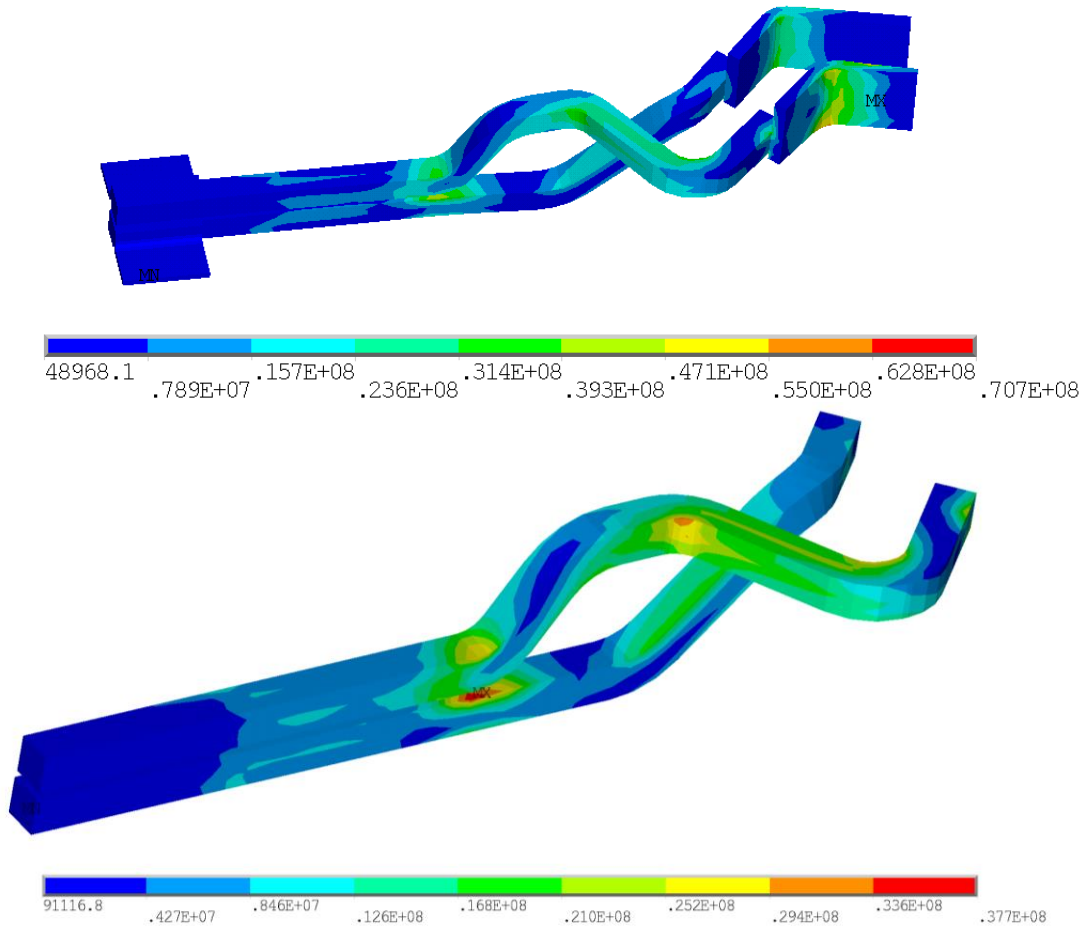


Fig 21.b Stress intensity in copper conductor [Pa]

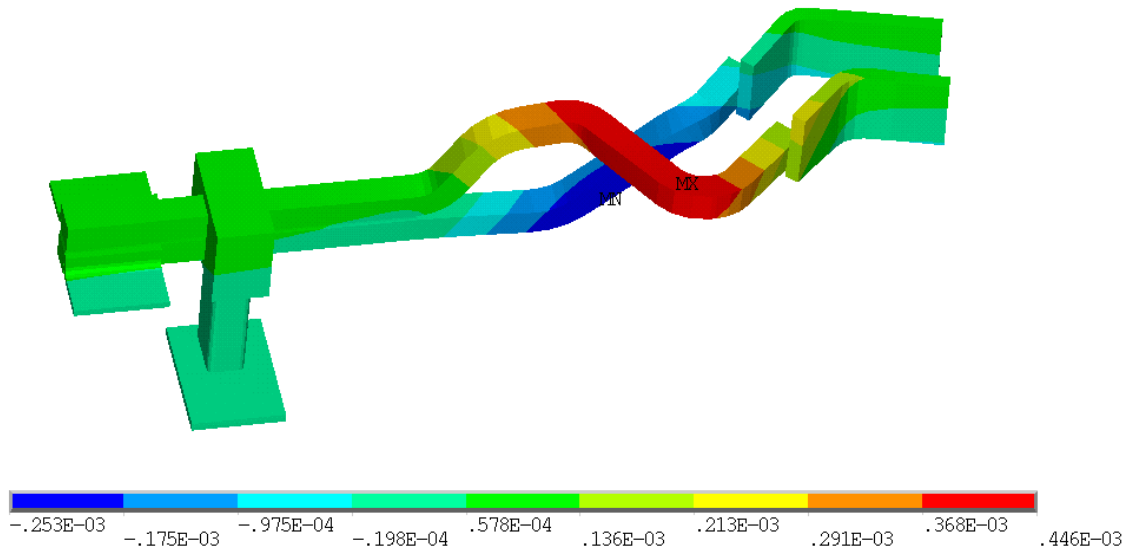


Fig 21.c Vertical Displacement [m]

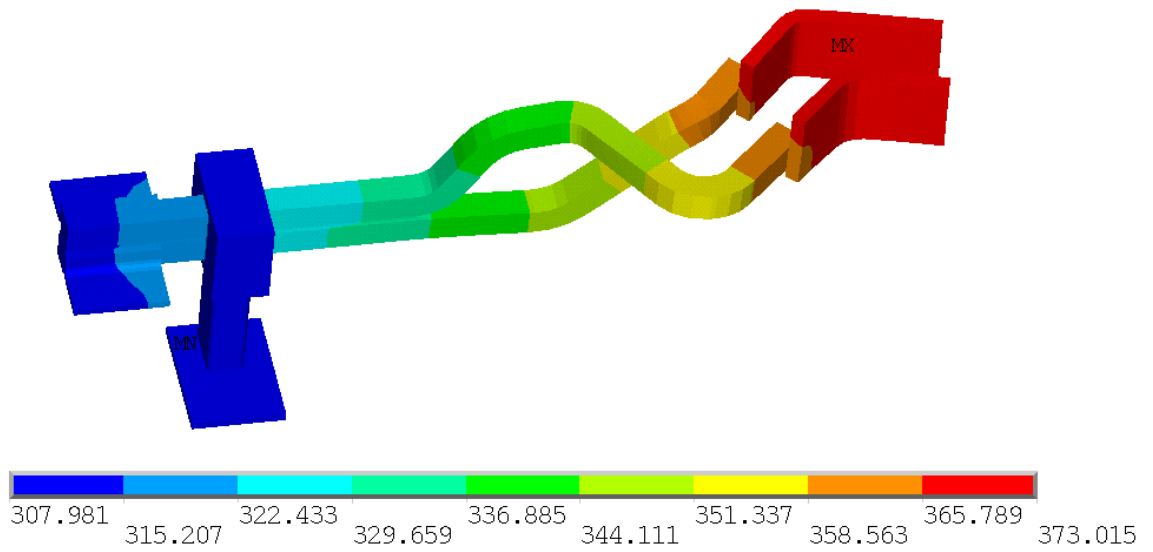


Fig 21.d Temperature [K]

PF Lower Bus Bars

PF1A Lower Bus Bar

Stress intensity and displacements on PF1A lower bus bar are presented on Fig. 22

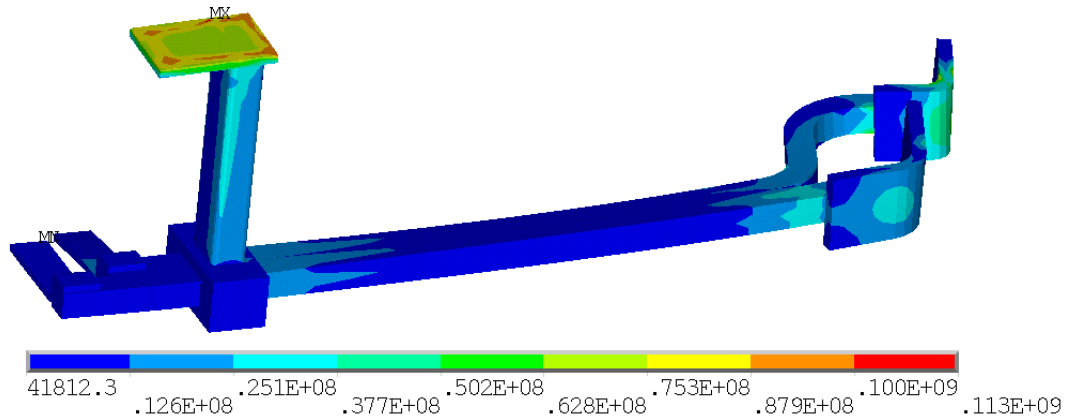


Fig 22.a Stress intensity [Pa]

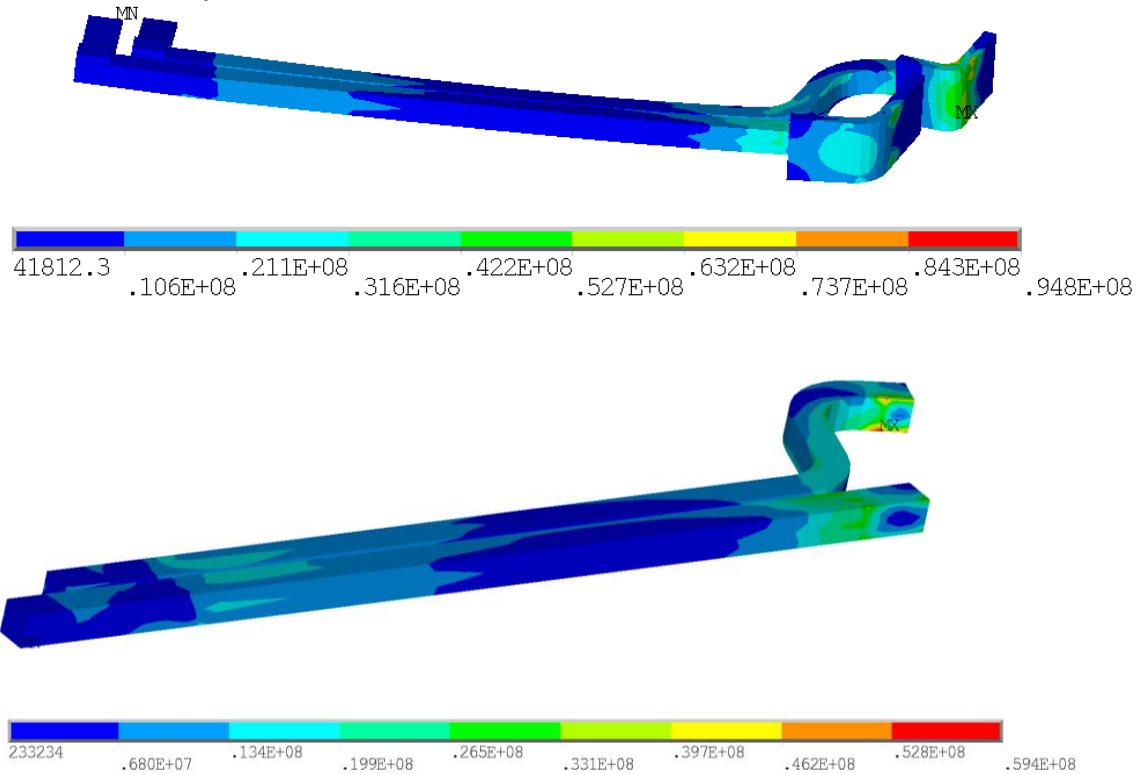


Fig 22.b Stress intensity in copper conductor [Pa]

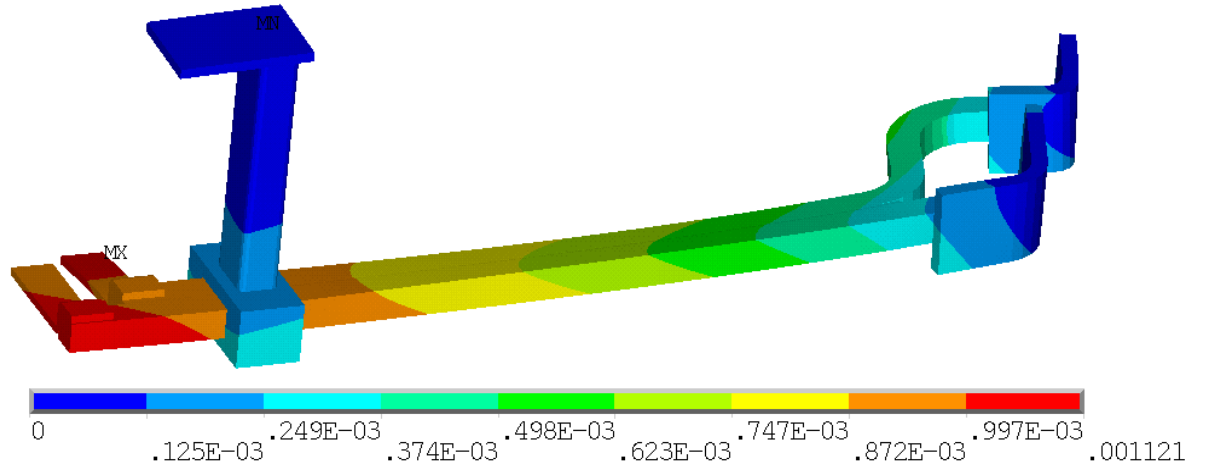


Fig 22.c Displacement [m]

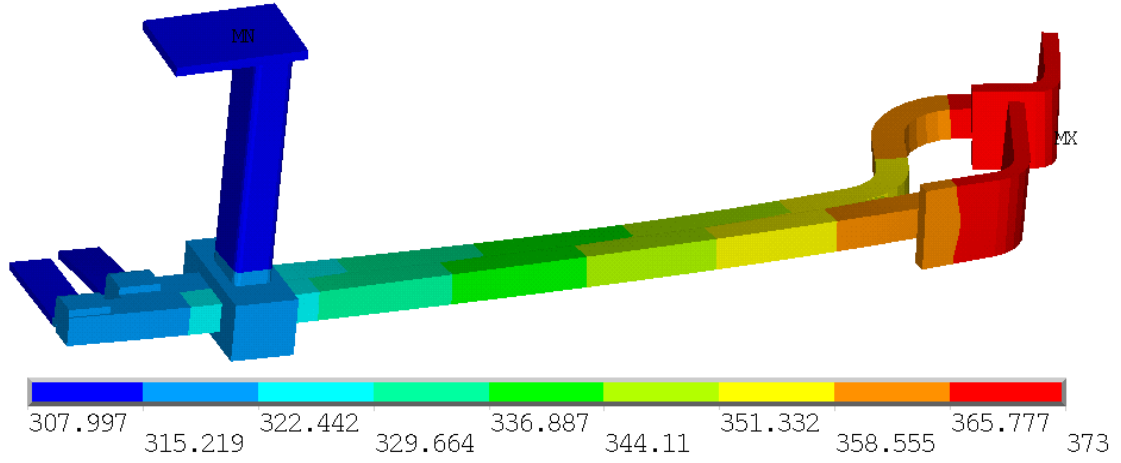


Fig 22.d Temperature [K]

PF1B Lower Bus Bar

Stress intensity and displacements on PF1B lower bus bar are presented on Fig. 23

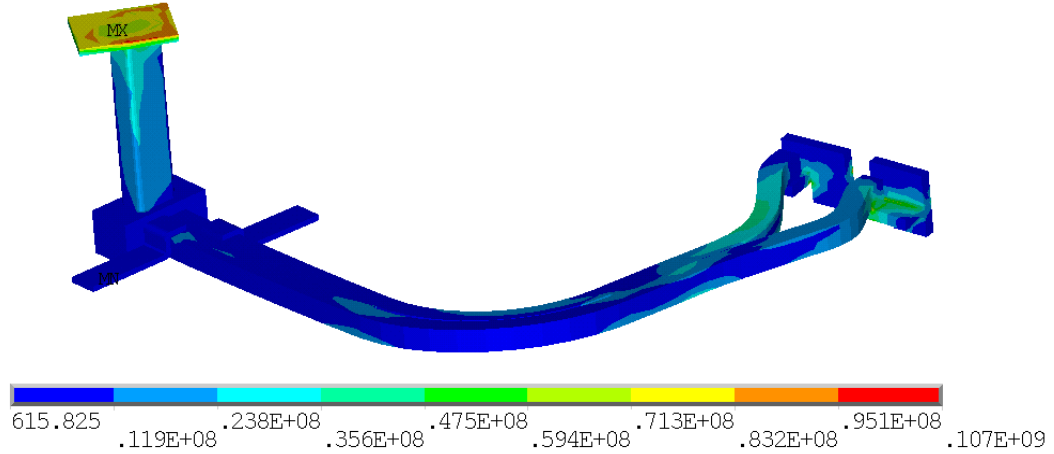


Fig 23.a Stress intensity [Pa]

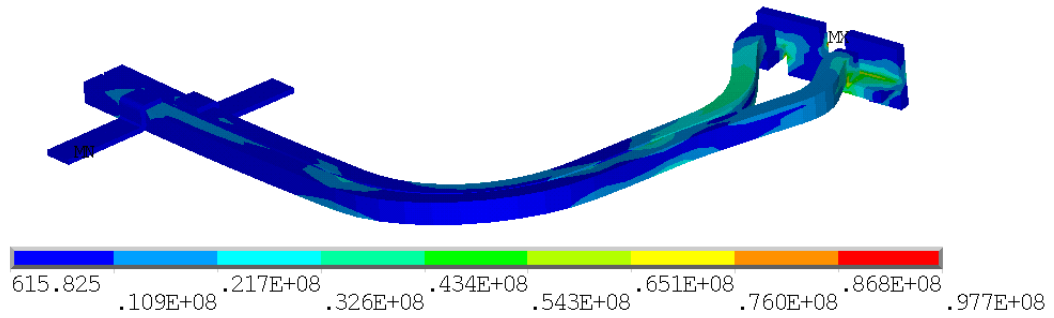
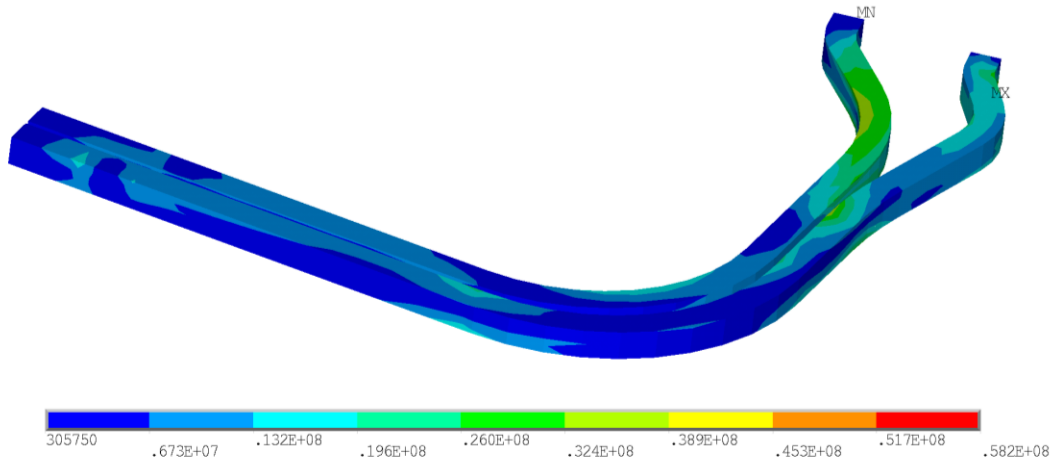


Fig 23.b Stress intensity in copper conductor [Pa]



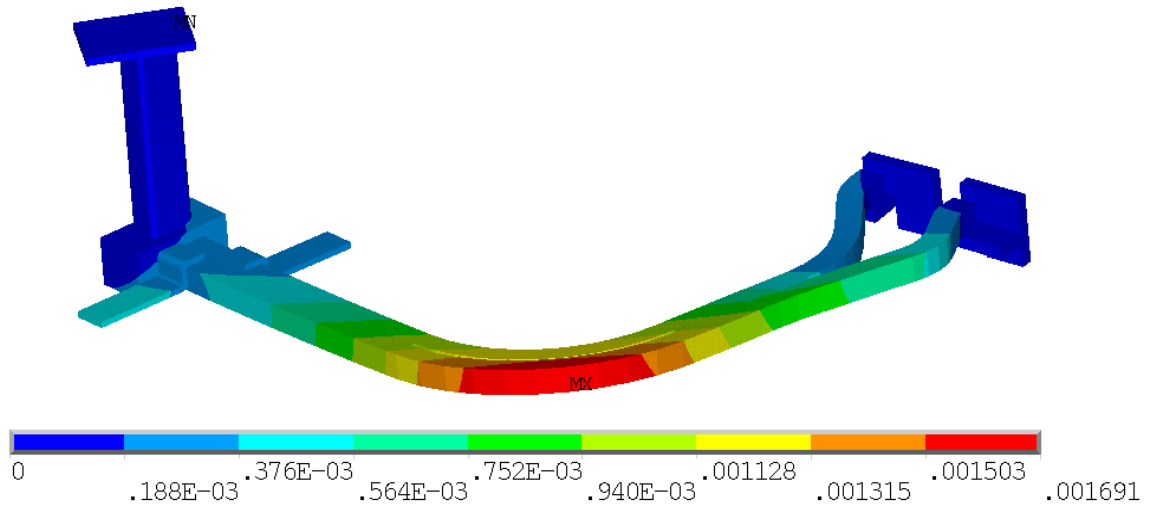


Fig 23.c Displacement [m]

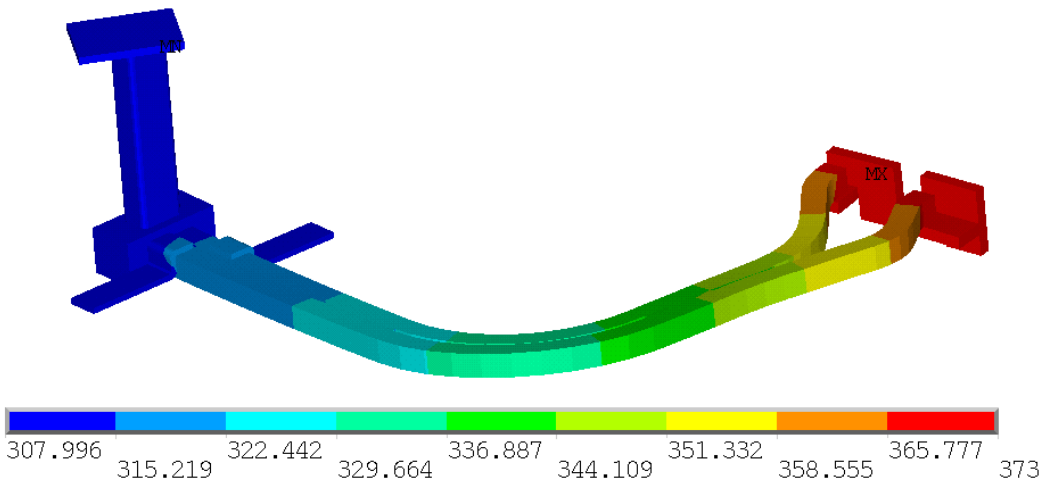


Fig 23.d Temperature [K]

PF1C Lower Bus Bar

Stress intensity and displacements on PF1C lower bus bar are presented on Fig. 24

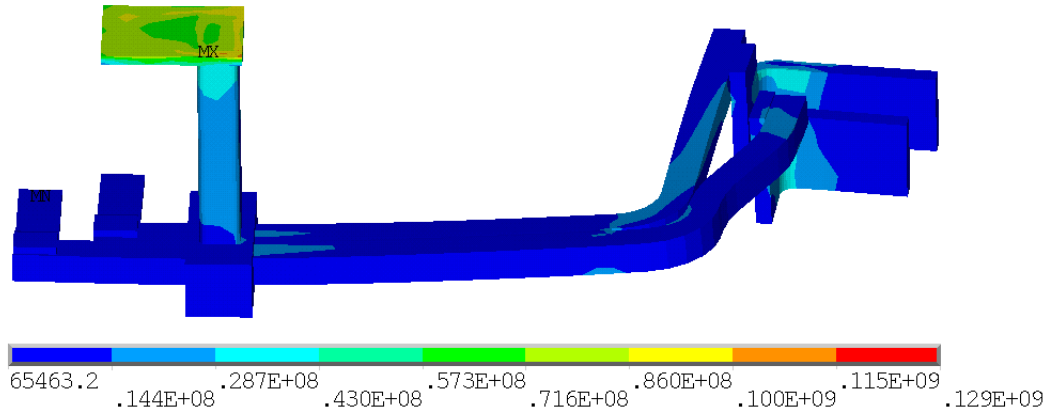


Fig 24.a Stress intensity [Pa]

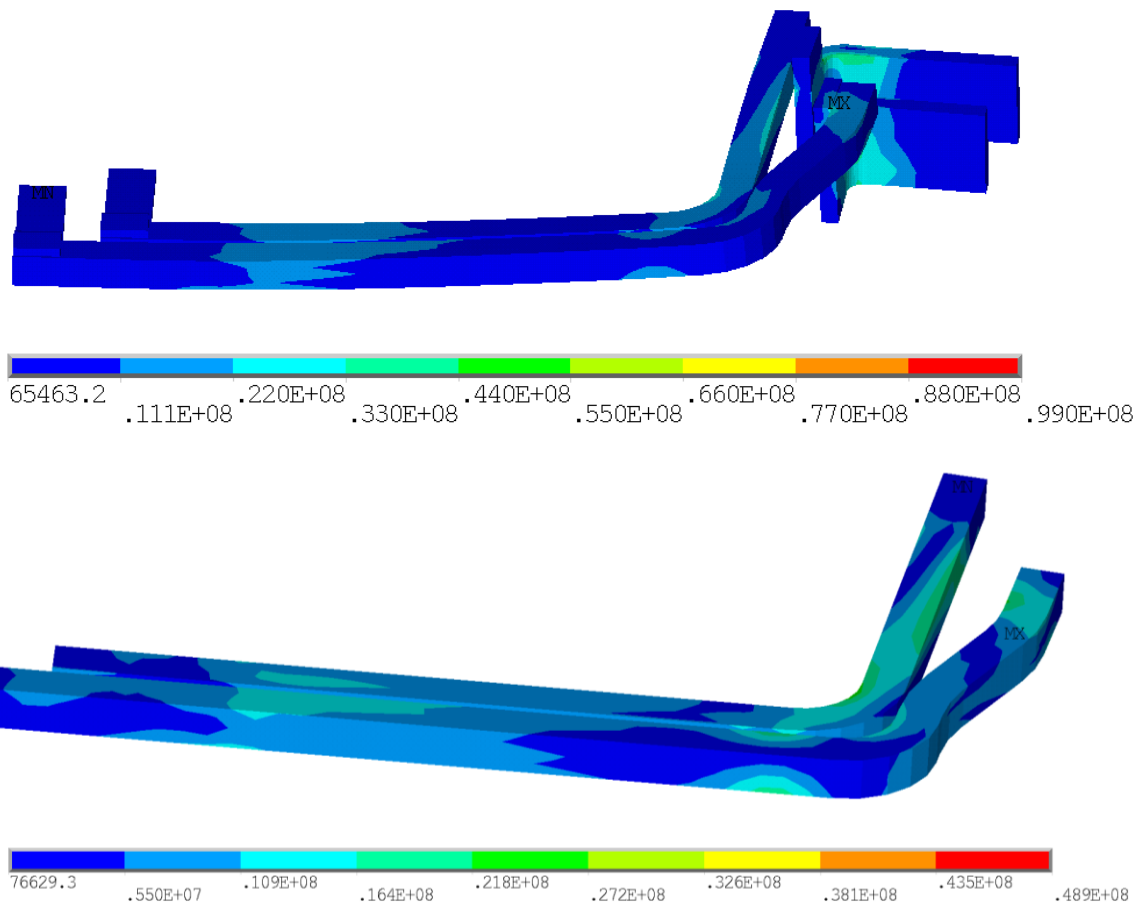


Fig 24.b Stress intensity in copper conductor [Pa]

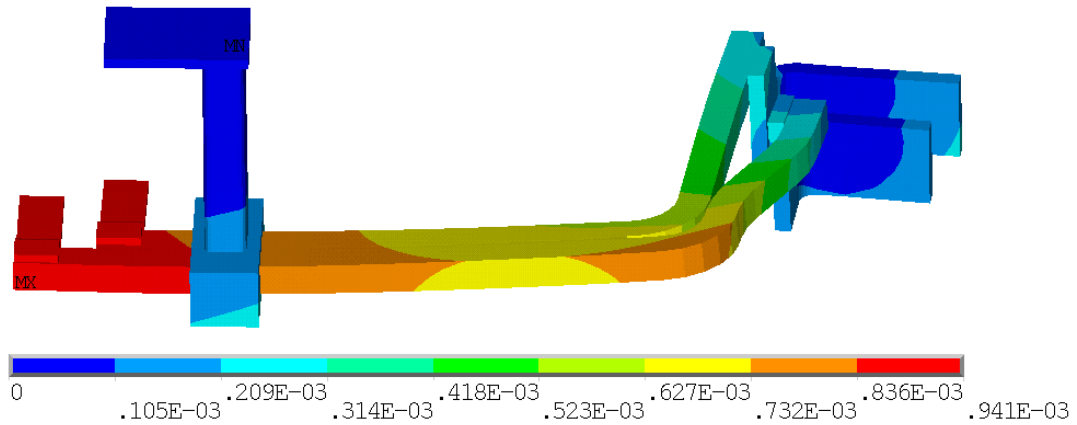


Fig 24.c Displacement [m]

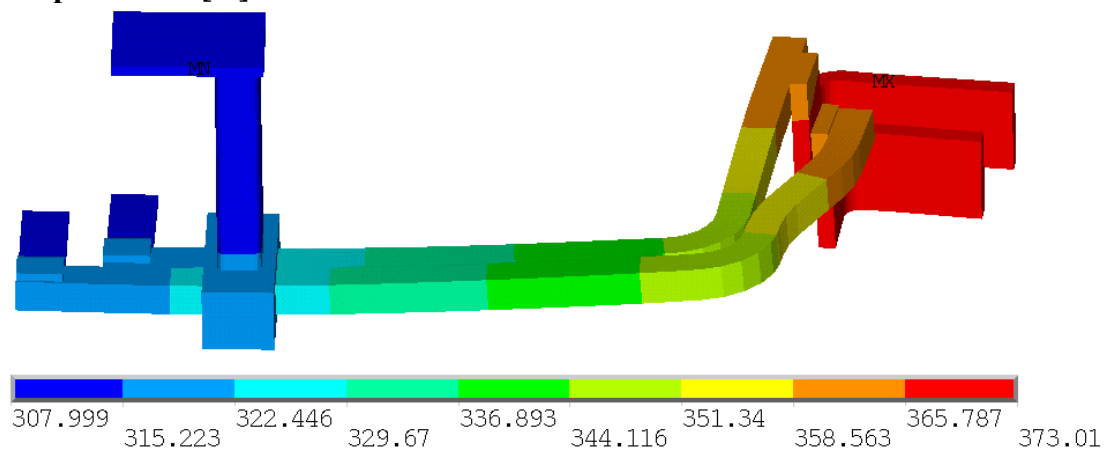
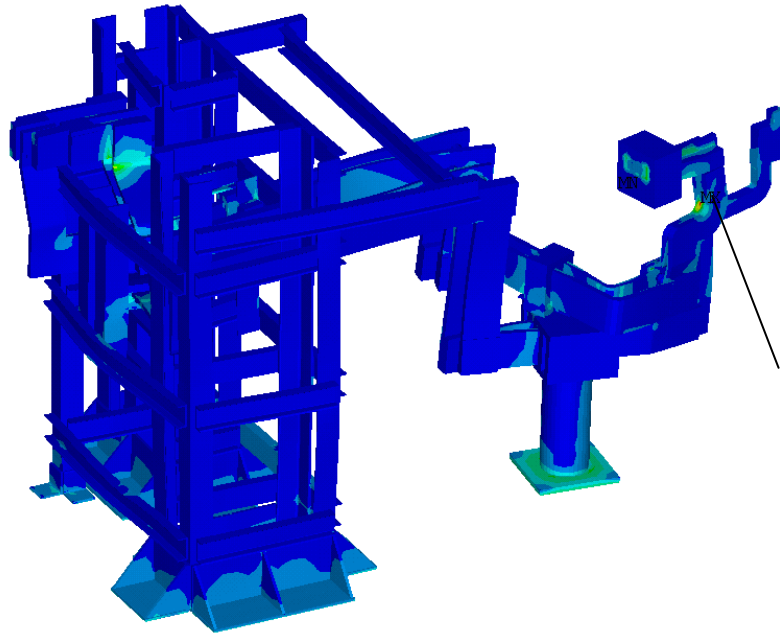


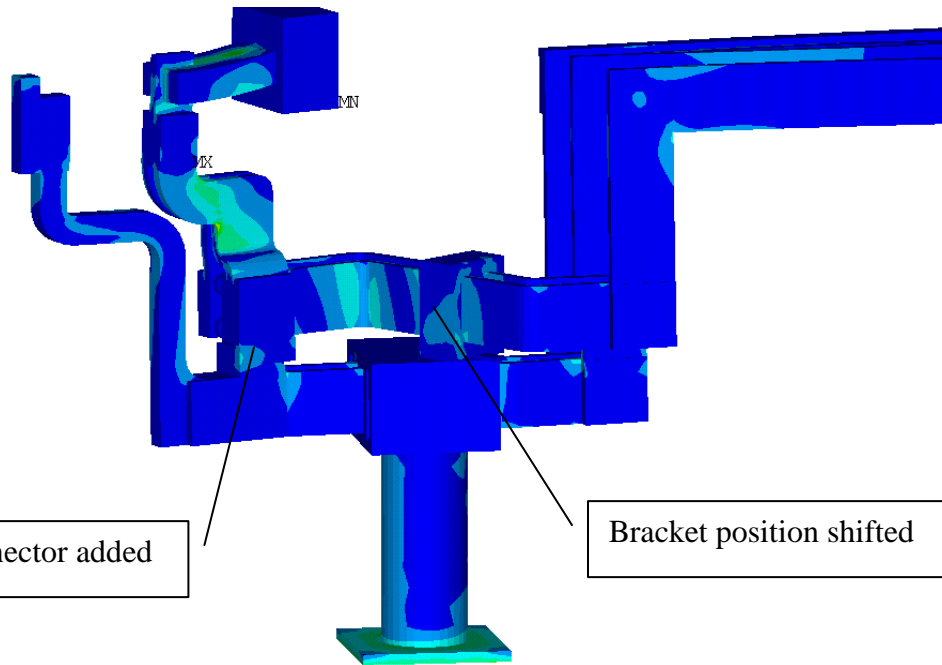
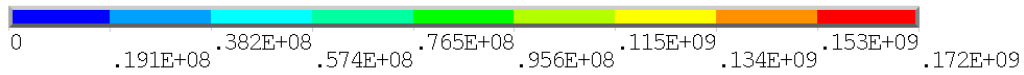
Fig 24.d Temperature [K]

TF Bus Bars

Stress intensity and displacements on TF bus bars are presented on Fig. 25. Figure 25.a shows peak stress intensity in copper near bolted connection between copper parts. Effect of friction in this connection was investigated by modeling the bolts with pretension and friction between the copper conductors. Figures 25.b and 25c show additional measures proposed to reduce stress intensity and displacement.



Effect of friction in bolted connection investigated for this joint



Insulating connector added

Bracket position shifted

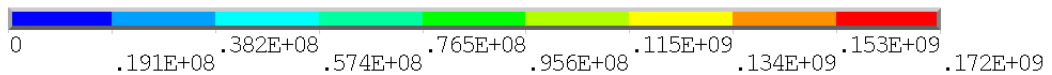


Fig 25.a Stress intensity [Pa]

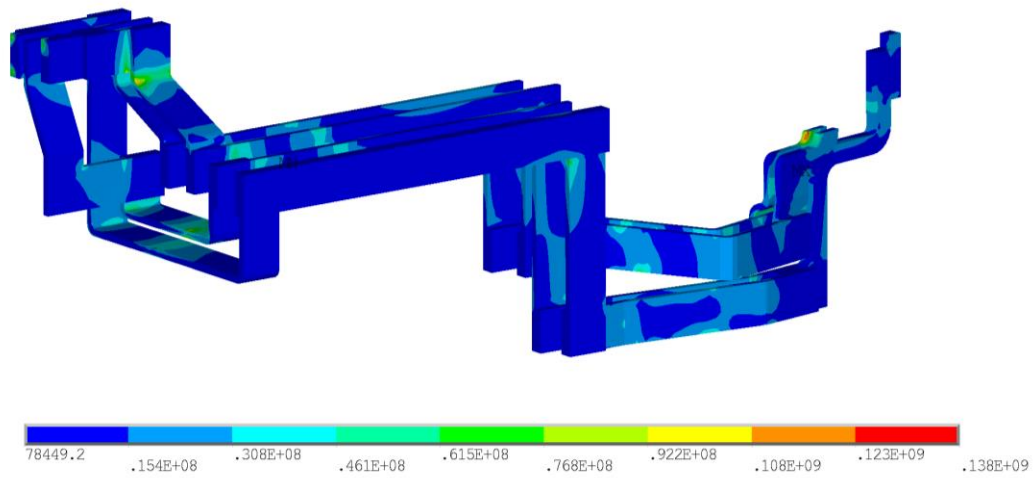


Fig 25.b Stress intensity in copper conductor [Pa]

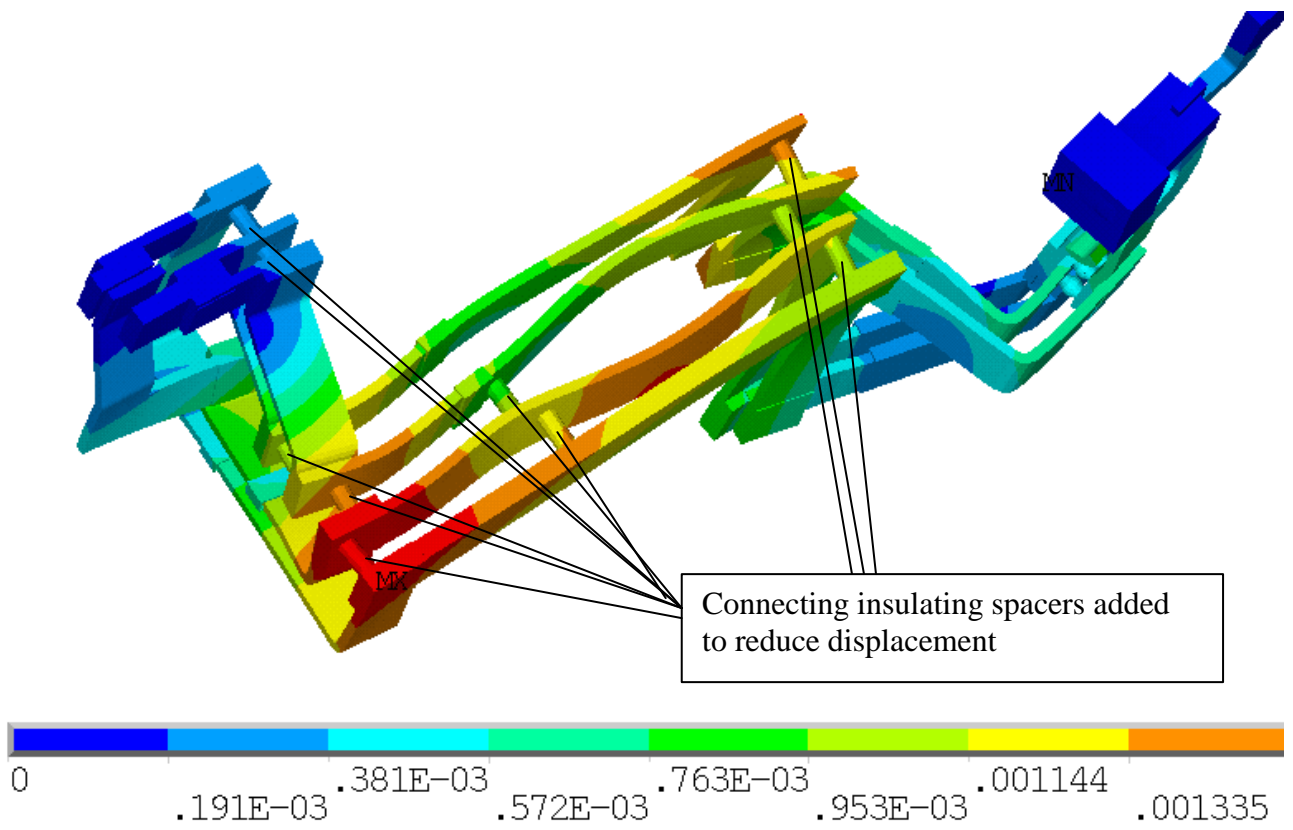


Fig 25.c Displacement [m]

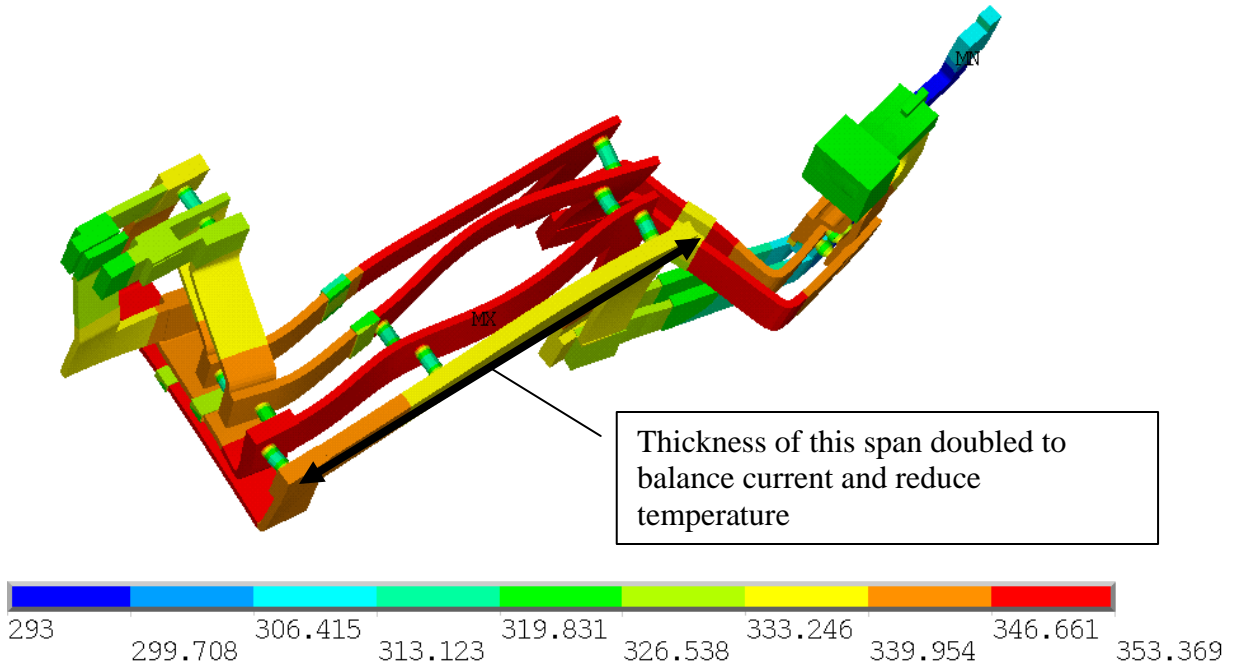


Fig 25.d Temperature [K]

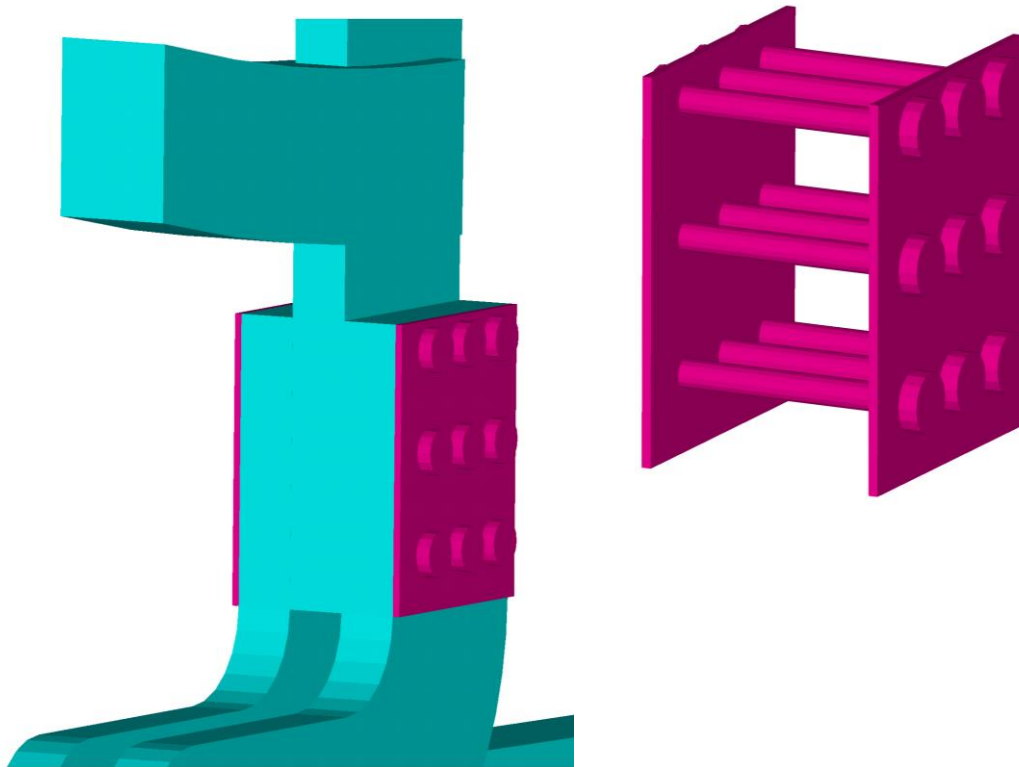


Fig 25.e Detailed model of bolted connection

NODAL SOLUTION
SUB =1
TIME=2
SZ (AVG)
TOP
RSYS=60
DMX =.002633
SMN =-.221E+09
SMX =.405E+09

ANSYS 14.5.7
PLOT NO. 1

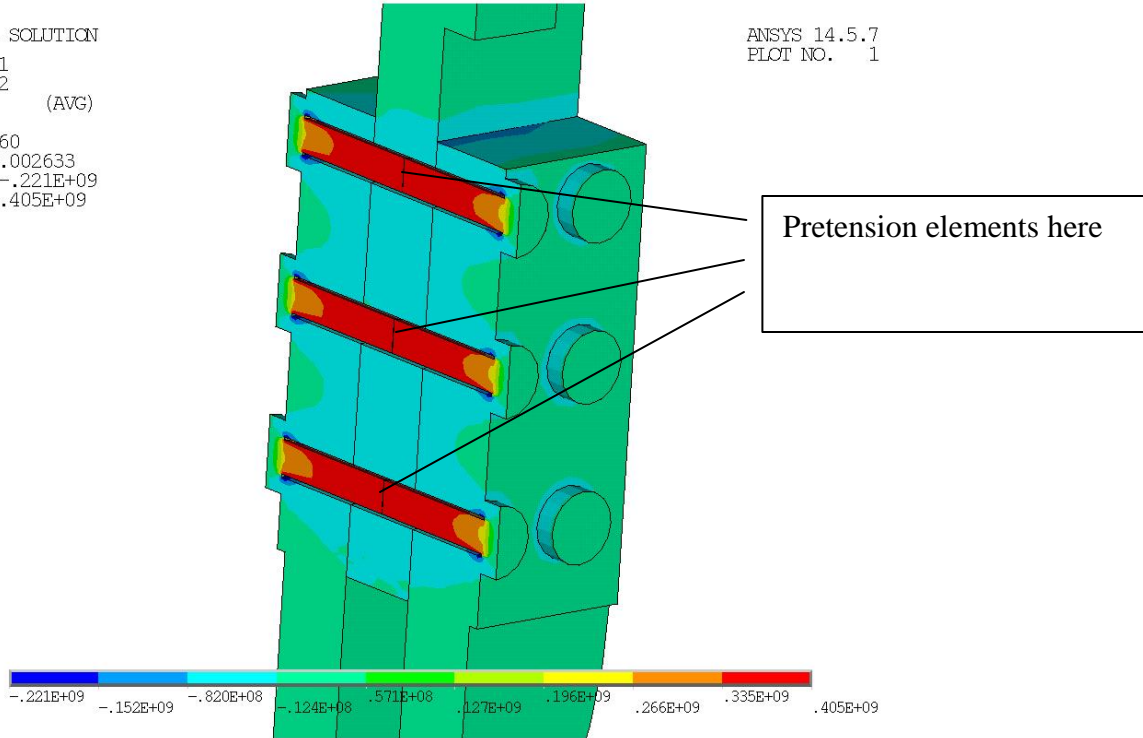


Fig 25.f Stress along the bolts in bolted connection cross-section [Pa]. Pretension 50ksi ~ 345MPa

NODAL SOLUTION
SUB =1
TIME=2
USUM
TOP
RSYS=60
DMX =.002633
SMX =.002633

ANSYS 14.5.7
PLOT NO. 1

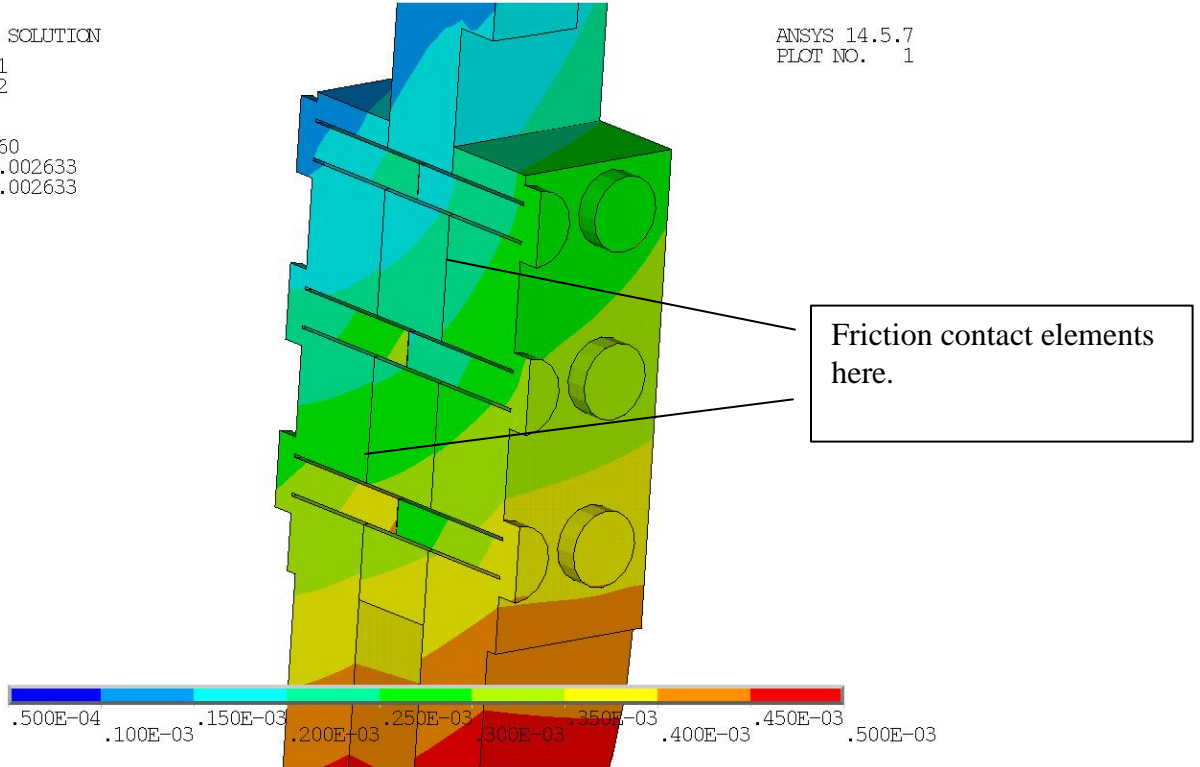


Fig 25.g Total displacement in bolted connection cross-section [m]. Friction coefficient 0.25

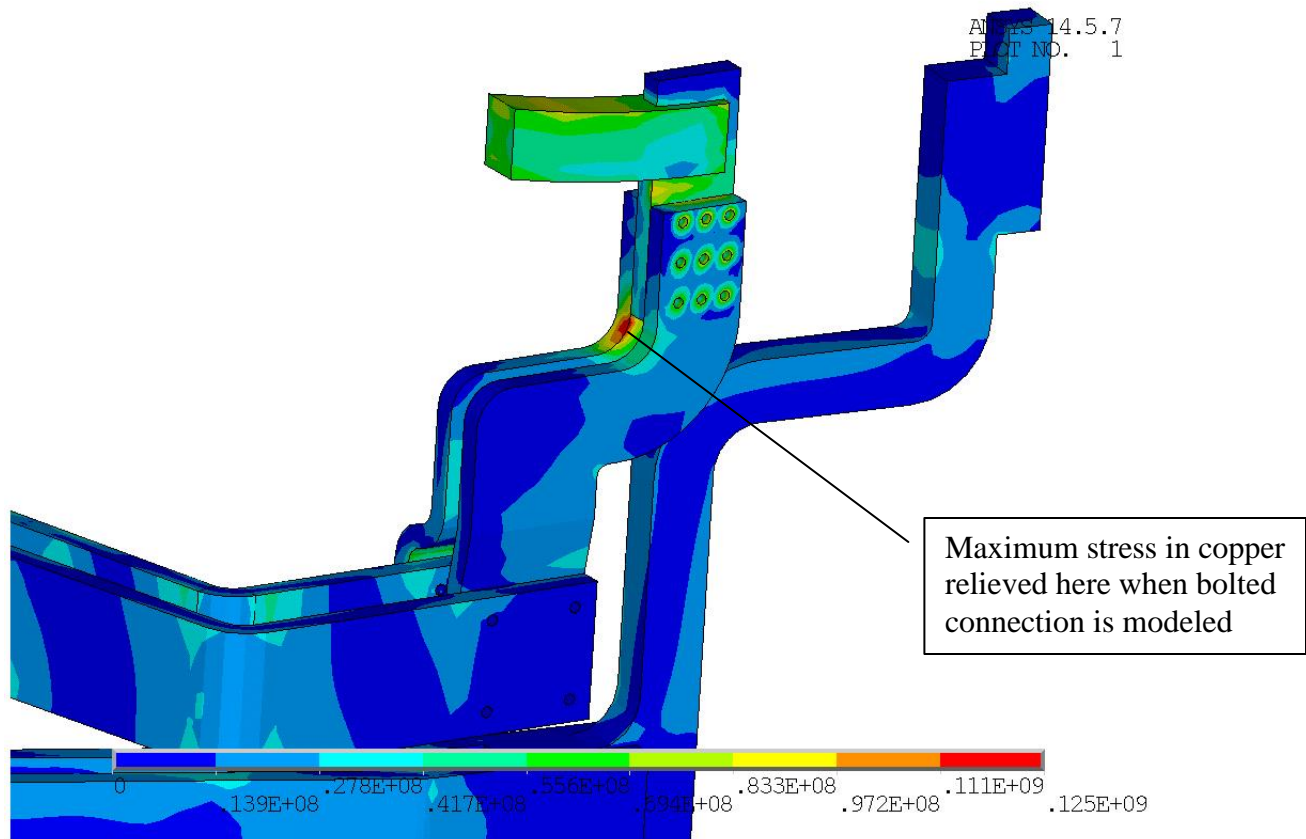


Fig 25.h Stress intensity [Pa] in copper near bolted connection. Friction coefficient 0.25

TIME=2
SINT (AVG)
TOP
RSYS=0
DMX =.002633
SMN =78449.2
SMK =.138E+09

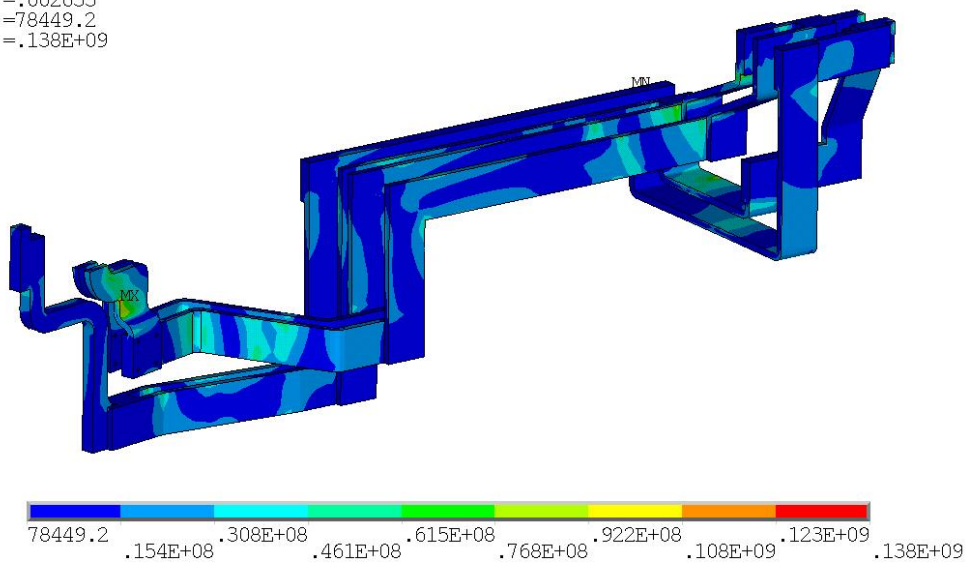
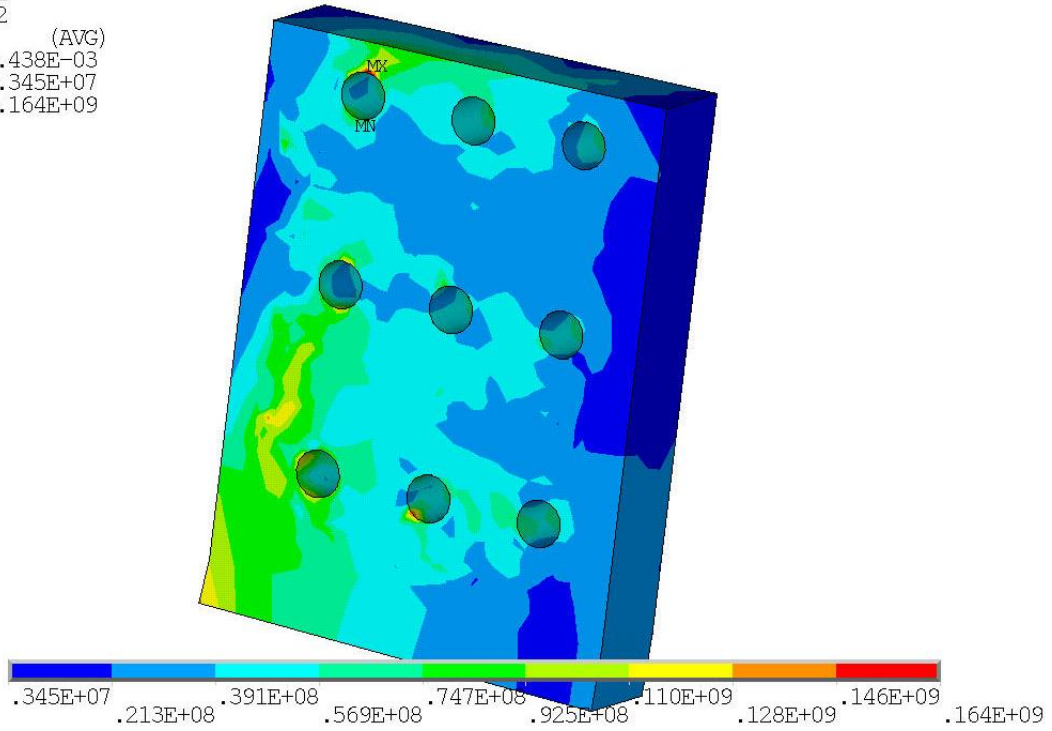


Fig 25.i Stress intensity [Pa] in copper when friction in bolted connection is included. Friction coefficient 0.25

TIME=2
SINT (AVG)
DMX = .438E-03
SMN = .345E+07
SMX = .164E+09



**Fig 25.j Stress intensity [Pa] in copper bolted connection when friction is included.
Friction coefficient 0.25**

NODAL SOLUTION
STEP=2
SUB =1
TIME=2
USUM (AVG)
RSYS=0
DMX = .453E-03
SMN = .945E-04
SMX = .453E-03

ANSYS 14.5.7
PLOT NO. 1

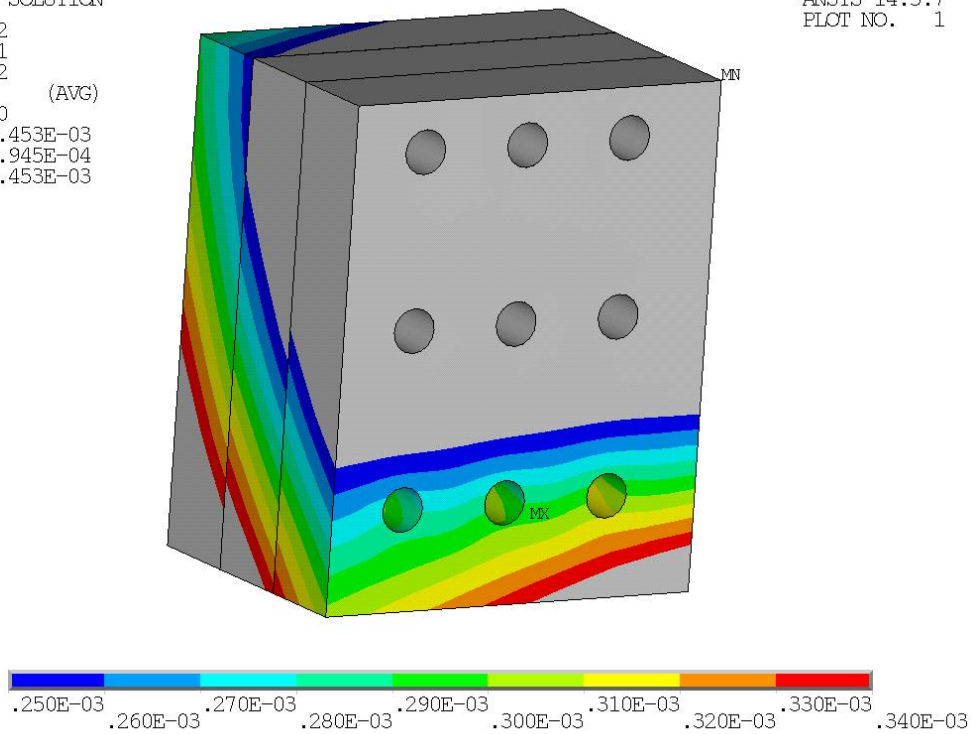


**Fig 25.h Displacement [m] in copper bolted connection when friction is included.
Friction coefficient 0.05**

Figure 25.e shows bolted connection modeled in detail to include effect of friction. Bolts were modeled like pretension rods. Connection between bolts nuts and stainless support plates is assumed bonded. Pretension PRETS179 elements are included in the bolts to create 50ksi pretension as shown on figure 25.f. Support plates are bonded to copper conductors. Node to node friction connection between copper conductors is established using CONTA178 elements as shown on fig 25.g. Friction coefficient is 0.1.

Results were obtained for values of friction coefficients of 0.05, 0.10, 0.015, and 0.025. Maximum stress in copper conductors is 137 MPa when friction coefficient is 0.05 and 138 MPa or all other values of friction coefficient. Location of the maximum stress intensity is presented on figure 25.i. Detailed modeling of the bolted connections leads to local maxima of stress intensity at the edges of the bolt holes on friction surfaces as shown on fig 25.j. These local values can be reduced using chamfer on the holes edges. Fig 25.h shows displacement in a bolted joint with friction coefficient of 0.005. Gaps in the iso-lines at friction surfaces show maximum displacement of around 0.01mm.

OH Bus Bars

Stress intensity and displacements on OH bus bars are presented on fig. 26

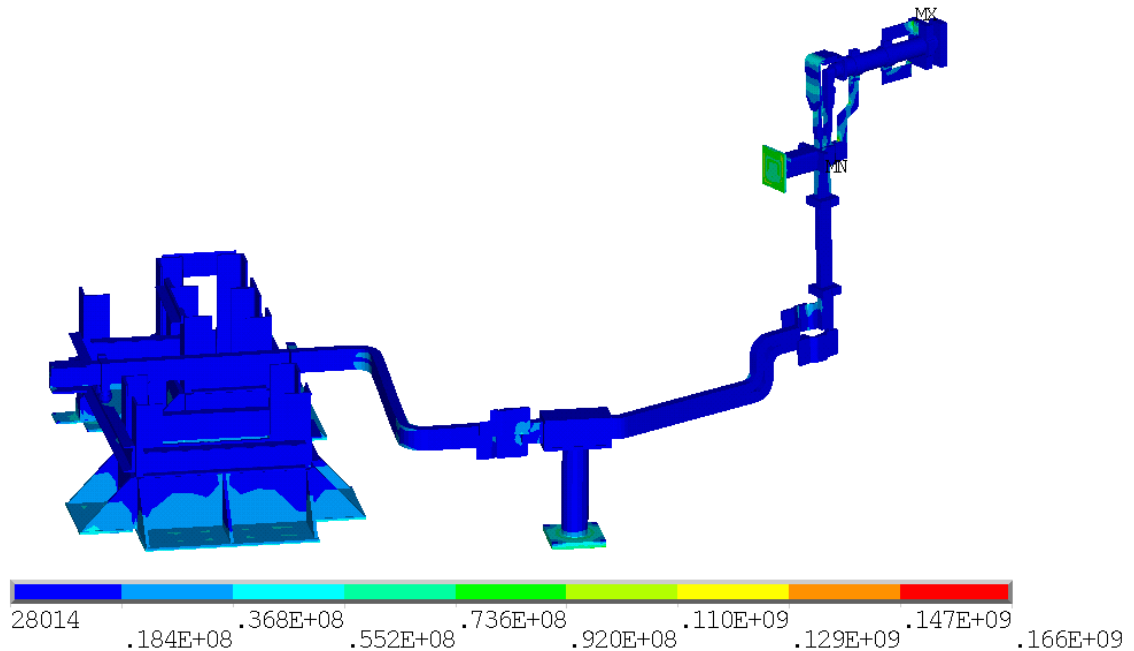


Fig 26.a Stress intensity [Pa]

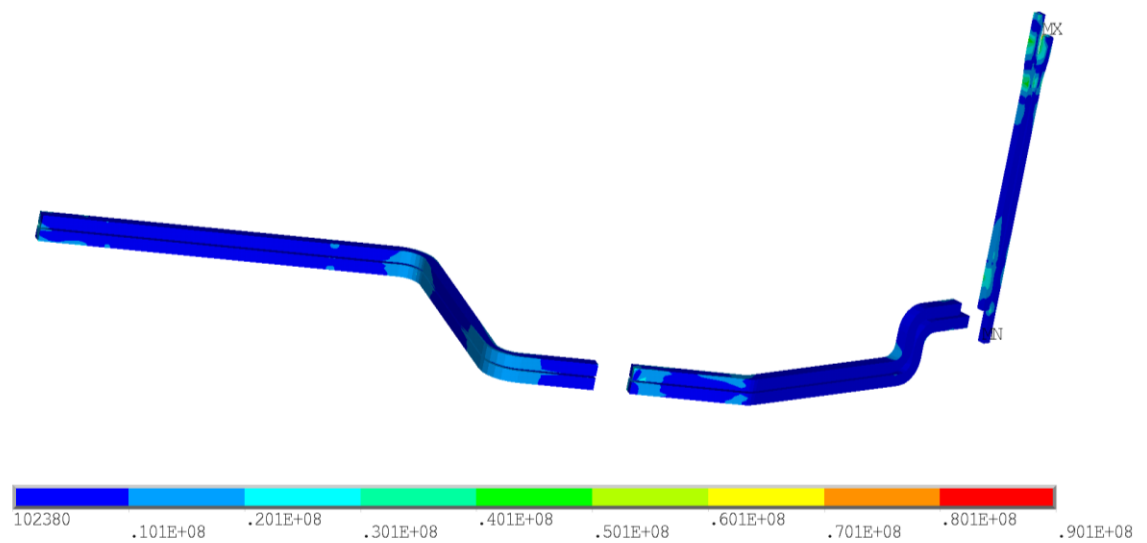
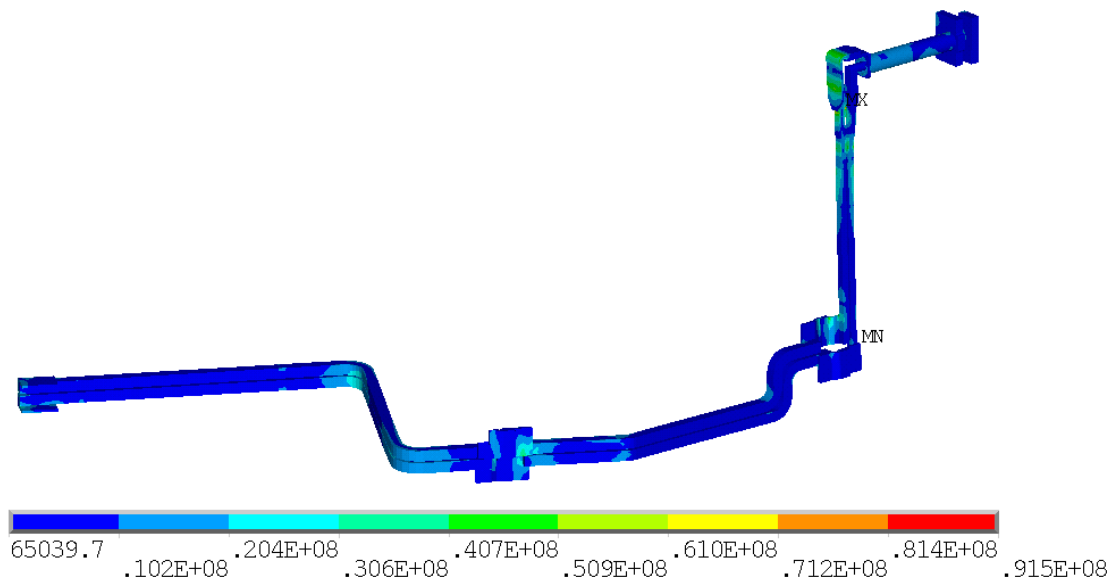


Fig 26.b Stress intensity in copper conductor [Pa]

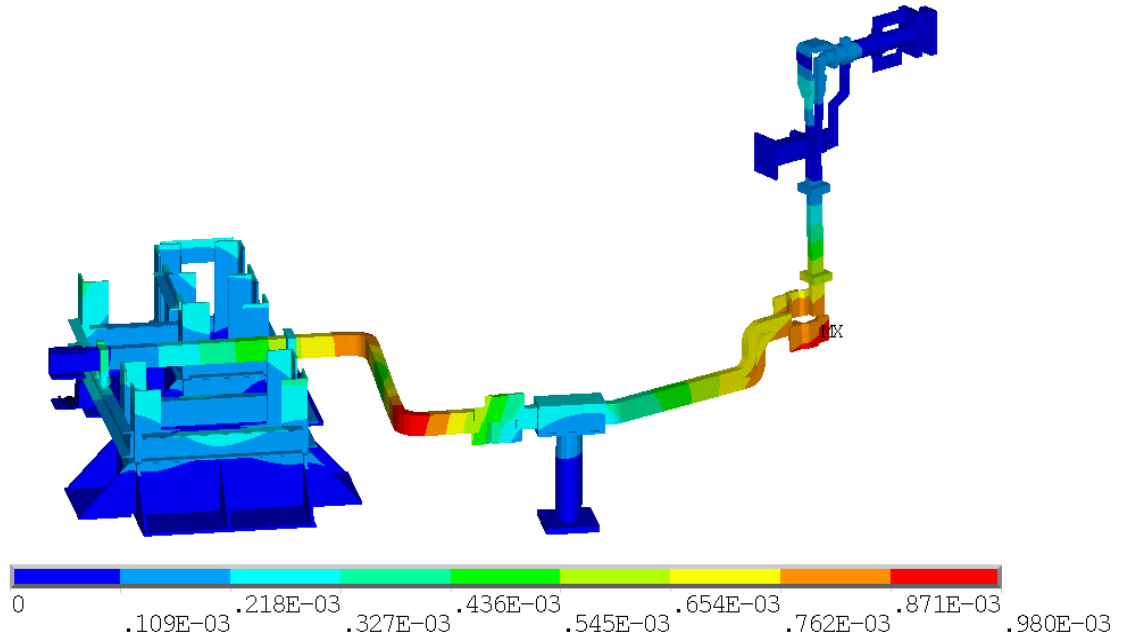


Fig 26.c Displacement [m]

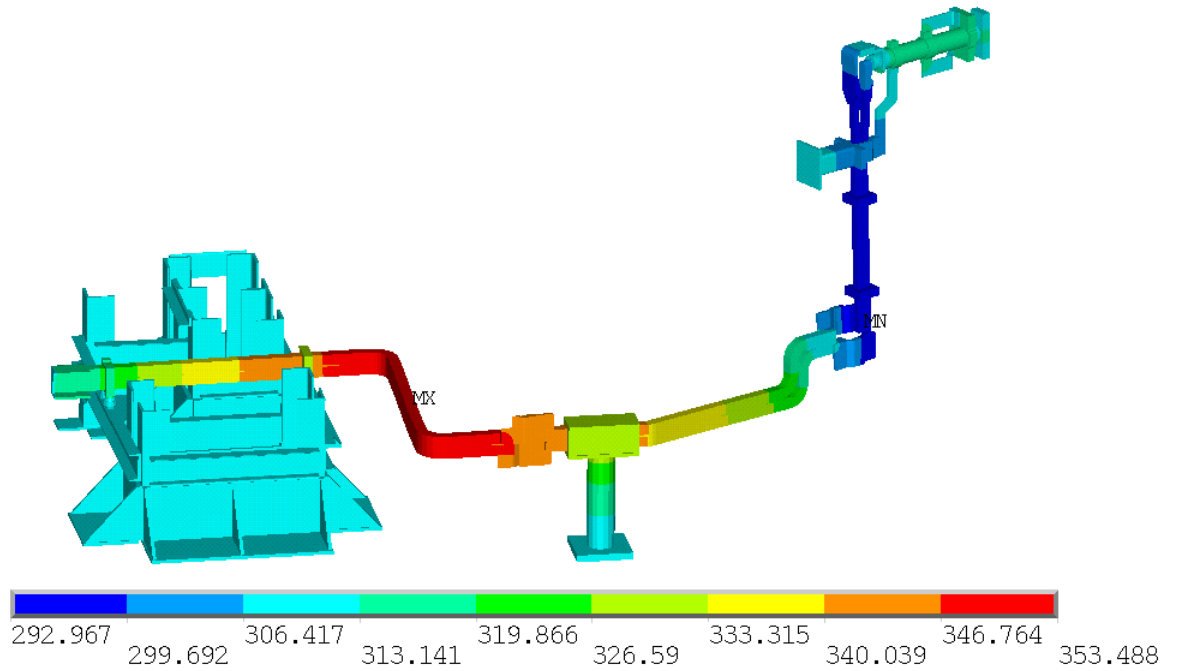


Fig 26.d Temperature [K]

Resistance of the Bus Bar Conductors

Resistance of the bus bar conductors is presented in table 6. It was obtained by dividing the corrected electric potential drop obtained in each conductor of the bus bar during numerical simulations by the current through the conductor. Electric potential drop was multiplied by the correction factor, which is used to correct resistivity in table 5. Location of each conductor of the bus bars is presented on fig 2.

Table 6 Resistance of bus bar conductors

Coil connected to Bus Bar	Conductor	Potential Drop [V]	Current [kA]	Resistivity Correction	Resistance [mΩ]
PF1A upper	1	0.00204	18.3	150	0.01675
PF1A upper	2	0.00206	18.3	150	0.01684
PF1B upper	1	0.00158	13	150	0.01818
PF1B upper	2	0.00159	13	150	0.01837
PF1C upper	1	0.00147	15.9	150	0.01382
PF1C upper	2	0.00166	15.9	150	0.01570
PF1A lower	1	0.00288	18.3	150	0.02358
PF1A lower	2	0.00262	18.3	150	0.02144
PF1B lower	1	0.00171	13	150	0.01971
PF1B lower	2	0.00186	13	150	0.02150
PF1C lower	1	0.00217	15.9	150	0.02047
PF1C lower	2	0.00227	15.9	150	0.02137
TF	1	0.01323	390	150	0.00509
TF	2	0.00909	390	150	0.00350
OH	1	0.01421	24	150	0.08882
OH	2	0.01448	24	150	0.09047

Outer OH Coax Terminal

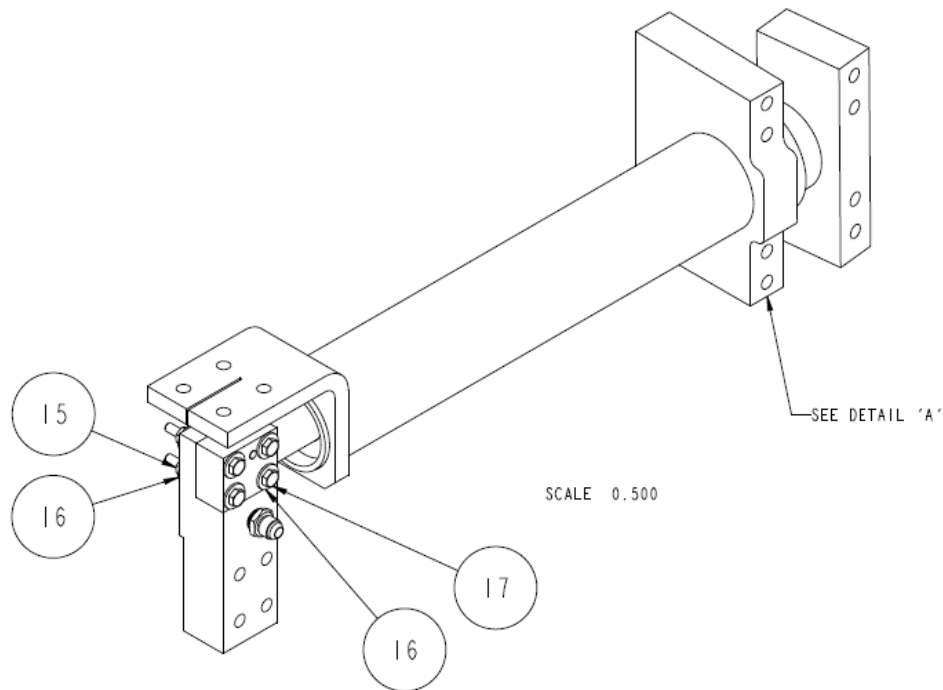
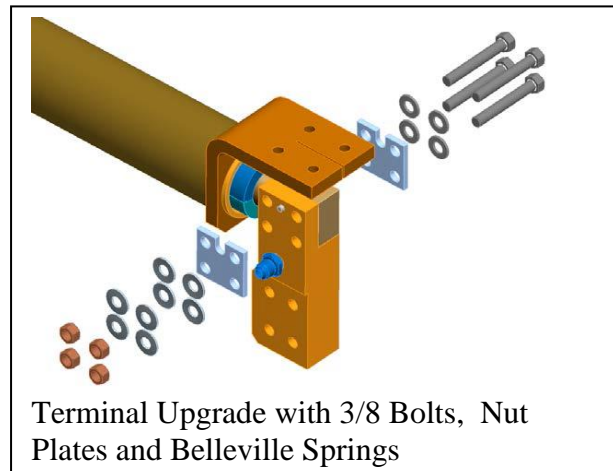
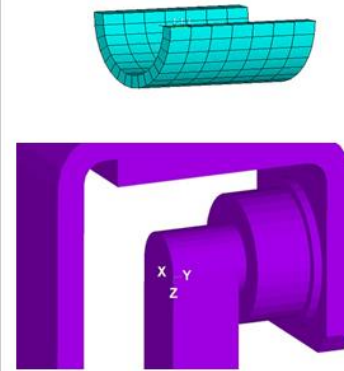
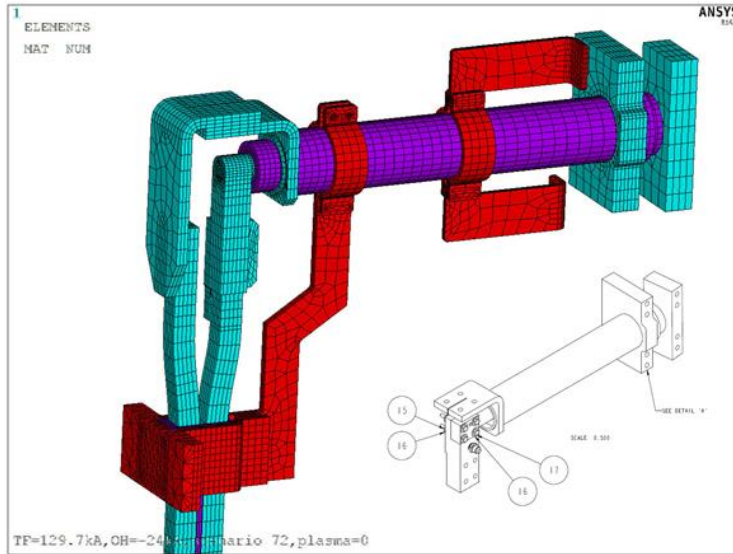


Fig 27 OH Coax with As-Built Rectangular Lap Joint

The braze joint, that was previously analyzed, was replaced with a bolted lap joint. With the brazed joint, the coax had to be assembled and then the outer flag brazed on to the inner conductor. To allow assembly of the inner and outer conductors of the coax independent of the outer connection braze, the inner conductor was terminated with a smaller block that allows insertion through the outer conductor tube. This allows assembly and tightening of the inner “feet” of the coax. Then the outer bolted lap joint is made-up and tightened. Then epoxy is injected in the annular spaces between the inner and outer conductors. Terminals can be adjusted slightly within the tolerances of the annular gaps and the epoxy fill process will not disturb the electrical contact at the terminals. This new process (as of June 2015) requires epoxy fill in-situ.

Loads at the outer terminal were extracted from the bus bar analysis. 1/4-20 bolts were specified at the lap joint. These provided insufficient contact pressure with the loads applied. They are being replaced with high strength 3/8 bolts. Note that the scope of this calculation is the connection of the coax to the bus bars. The coax and its inner connections are qualified in [6]

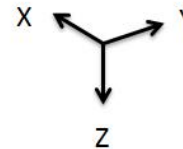




*** NOTE *** CP = 143.490 TIME= 14:38:11
 Summations based on final geometry and will not agree with solution reactions.

***** SUMMATION OF TOTAL FORCES AND MOMENTS IN COORDINATE SYSTEM111
 NOTE: THE SUM IS DONE IN COORDINATE SYSTEM111
 FX = 28.07885
 FY = 934.0658
 FZ = -1935.135
 MX = -768.9637
 MY = 43.50109
 MZ = 10.51664
 HEAT= 20.22263
 AMPS= 17823.76
 FLUX= 0.1018815E-03

Forces in Newtons and Moments in Newton-Meter



SUMMATION POINT= 0.0000 0.0000 0.0000

Fig 28 Loads at the Outer Terminal of the OH Coax Joint

The 3/8 bolts are preloaded to 43.5 ft-lbs which produces a tensile load of 6957 lbs per bolt and an average pressure of 9 ksi on the terminal face. Belleville springs are added to help maintain the preload. The bolt stress is 90 ksi at this torque level and Inconel 718 bolts with a yield of greater than 100ksi are specified. With a friction coefficient, the shear load capacity is $6957 * 4 * .3 = 8348$ lbs, or 37kN - much much larger than the loads applied. The moment about the X axis is more challenging. If just the “clutch face” frictional torque capacity resists M_x , then the x moment can't be supported. But the lug is tightly fitted in the recess that forms the lap. Taking credit for bearing at this surface, the moment can be supported with a factor of safety of 1.89. Figure 29 shows the calculations with and without the bearing at the fit edge. The NSTX Structural Criteria [2] requires a +/- .15 range on the friction coefficient. If the friction coefficient were as low as .15, the frictional margin would drop slightly below 1, but the bolts would load directly in shear to make up the difference.

[6] OH Coaxial Cable and Embedded Leads NSTXU-CALC-133-07-00 10 M.
Mardenfeld October 2011